PHYSICAL REVIEW
LETTERS

VOLUME 5 NOVEMBER 1, 1960 NUMBER 9

INSTABILITY OF A POSITIVE COLUMN IN A MAGNETIC FIELD*

T. K. Allen,† George A. Paulikas,‡ and Robert V. Pyle
Lawrence Radiation Laboratory, University of California, Berkeley, California
(Received September 26, 1960)

The particle and energy losses from a long positive column of a helium glow discharge were shown by Lehnert[1] to decrease with increasing longitudinal magnetic field as predicted by ambipolar diffusion theory, but only for fields less than a critical field, B_c. Above B_c the losses increased, leading to speculation about the possibility of "enhanced diffusion." Further measurements by Lehnert and Hoh,[2] and at this laboratory, extended Lehnert's measurements to other gases and discharge tube parameters; in particular, it was shown[3] that at B_c the discharges lose their azimuthal symmetry and appear as constricted, rotating, luminous helices (Fig. 1). In addition to the critical magnetic fields, the wavelengths and oscillation frequencies of such helices have now been measured for a number of discharge conditions. In this Letter the experimental results are compared with the two existing theories[4,5] and are shown to be in reasonable agreement with one of them.[5]

Recently, Hoh[4] and Kadomtsev and Nedospasov[5] have considered the origin of the instability from two different standpoints. Hoh made use of a criterion for the stability of a wall sheath and showed that it is no longer satisfied when the magnetic field exceeds a critical value. The manner in which the failure of the sheath-stability criterion affects the discharge was not discussed. Kadomtsev and Nedospasov, on the other hand, show that perturbations of the discharge column can grow when diffusion to the walls can no longer overcome the effects of $\vec{j}\times\vec{B}$ forces that tend to increase the perturbation. $\vec{j}$ cannot be zero, but the value of B_c obtained does not depend on the magnitude of the current density. In addition to predicting B_c, their theory predicts the frequency, wavelength, and growth rate of the oscillation.

In our experiment, discharge tubes 250 cm long were placed at the axis of a solenoid which could be adjusted in length up to 200 cm. As in references 1 and 2, the discharges were run at constant current, and the axial field was used as a measure of particle losses. These fields were obtained from a number of probes. The time and space variations of the visible light from the dis-

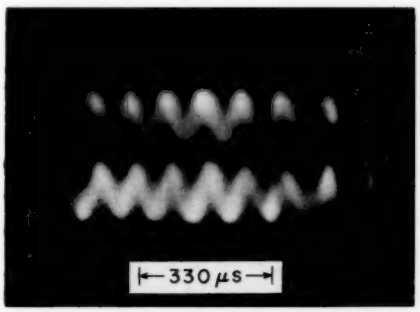

FIG. 1. 90-degree stereo streak photograph of helical constriction in helium. $R = 2.75$ cm, $p = 0.23$ mm Hg, $B = 710$ gauss. Traces show variation of light intensity with time and radius as seen through a slit perpendicular to axis of discharge tube. Note that this is not a photograph of the helix; the helicity has been established by wavelength measurements with photomultipliers.

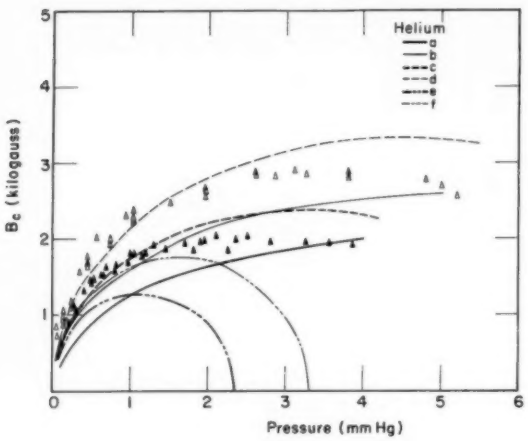

FIG. 2. The critical magnetic field, B_c, vs gas pressure. ▲: $R = 1.27$ cm, $I = 400$ ma; Δ: $R = 0.9$ cm, $I = 200$ ma. (a) $R = 1.27$ cm and (b) $R = 0.9$ cm, calculated from Kadomtsev's theory. (c) $R = 1.27$ cm and (d) $R = 0.9$ cm, calculated from Hoh's theory, assuming only He_2^+ ions present. (e) $R = 1.27$ cm and (f) $R = 0.9$ cm, from Hoh's theory, assuming only He^+ ions present.

charge were photographically recorded from a rotating mirror and a series of well-collimated photomultipliers. From the measurements it was possible to obtain data on the critical magnetic fields and the oscillation frequencies, wavelengths, and growth rates for H_2, D_2, He, Ne, and A in tubes with radii of 0.9, 0.95, 1.27, and 2.75 cm.

Luminous helices of the clarity shown in Fig. 1 were observed only for special combinations of gas, pressure, and tube radius. In general, the appearance was more chaotic, often appearing as moving striations superimposed on the spirals. The pitches of the spirals were such that $\vec{j} \times \vec{B}$ was directed toward tube walls.

Some of the experimental B_c vs p data are shown in Figs. 2 and 3, together with calculations from the formulas[6] of references 4 and 5. Numerical data were taken from the compilation by Brown.[7] Considerable uncertainty exists as to the actual conditions in a positive column, e.g., both atomic and molecular ions are known to be present. The predictions of the sheath theory are not particularly sensitive to temperature, but depend critically on the mobilities; we show calculated curves for two ionic species to illustrate the latter point. On the other hand, the results of the current-channel instability theory depend much more sensitively on temperature than on mobility, B_c varying roughly as T_e for a given pressure. The moving striations that were generally present in our discharges may appreciably affect the electron energy distribu-

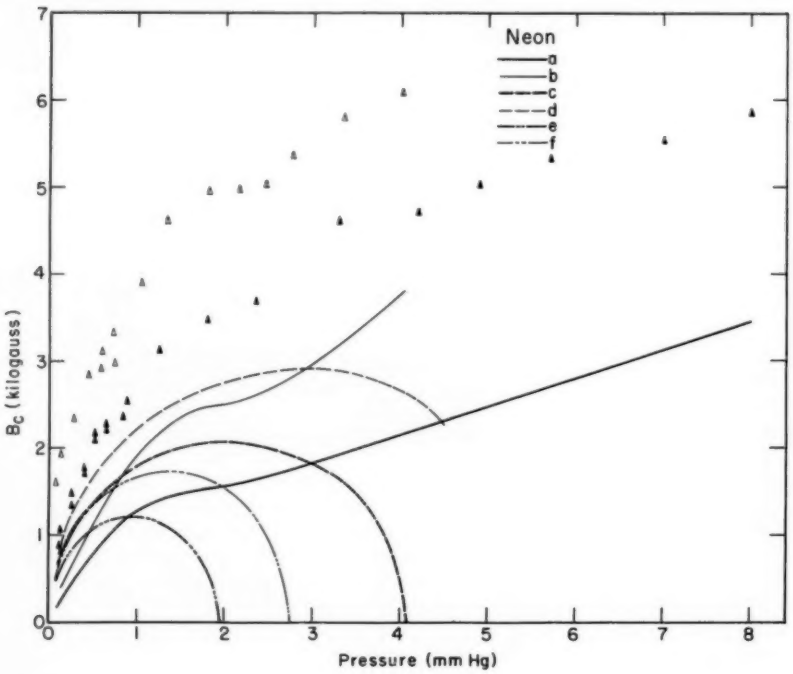

FIG. 3. The critical magnetic field, B_c, vs gas pressure. ▲: $R = 1.27$ cm, $I = 400$ ma; Δ: $R = 0.9$ cm, $I = 200$ ma. (a) $R = 1.27$ cm and (b) $R = 0.9$ cm, calculated from Kadomtsev's theory. (c) $R = 1.27$ cm and (d) $R = 0.9$ cm, calculated from Hoh's theory, assuming only Ne_2^+ ions present. (e) $R = 1.27$ cm and (f) $R = 0.9$ cm, from Hoh's theory, assuming only Ne^+ ions present.

tions, although the B_C vs p curves go smoothly through transitions from unstriated to striated regimes. Similar uncertainties exist for the H_2, D_2, and A discharges.

Where it was possible to obtain oscillation frequencies and wavelengths from the experimental results, these quantities were in good agreement with values obtained from the formulas in reference 5. For example, helium at 0.3 mm Hg pressure in a 2.75-cm radius tube gave an angular frequency of 5×10^4 radians/sec and a wavelength of 73 cm, the calculated values being 4.3×10^4 and 63, respectively.[8] In addition, the frequencies increased with decreasing radius and decreasing pressure, as predicted in Eq. (22) of reference 5. Growth rates were difficult to determine experimentally, but showed agreement in order of magnitude.

We conclude that with the proper choice of parameters either theory can approximate the experimental B_C vs p curves, although the shapes of the latter are perhaps most like the results of Kadomtsev and Nedospasov. Their theory also yields perturbation frequencies and wavelengths in good agreement with experiment.

We wish to thank C. M. van Atta for supporting this research, J. Warren Stearns for helping with many of the measurements, Y. T. Fung, L. S. Hall, and W. B. Kunkel for discussions of the theory and experiment, H. S. Powell for the glass blowing, and many members of William R. Baker's Sherwood research group for aid in construction of the apparatus.

---

*Work was performed under the auspices of the U. S. Atomic Energy Commission.

†Atomic Energy Research Establishment, Harwell, England.

‡National Science Foundation Fellow.

[1]B. Lehnert, Proceedings of the Second International Conference on the Peaceful Uses of Atomic Energy (United Nations, Geneva, 1958), Vol. 32, p. 349.

[2]B. Lehnert and F. C. Hoh, Phys. Fluids 3, 600 (1960).

[3]T. K. Allen, G. A. Paulikas, and R. V. Pyle, Bull. Am. Phys. Soc. 5, 314 (1960).

[4]F. C. Hoh, Phys. Rev. Letters 4, 559 (1960).

[5]B. B. Kadomtsev and A. V. Nedospasov, J. Nuclear Energy Part C 1, 230 (1960). We are grateful to the authors for a prepublication copy of this paper.

[6]Equation (4) of reference 4 has apparently been misprinted; the second quantity in brackets should read $(g'p_0\lambda/R-p_0^2)^{1/2}$.

[7]S. C. Brown, Basic Data of Plasma Physics (John Wiley & Sons, Inc., New York, 1959).

[8]The experimental frequencies and wavelengths were obtained from the fully developed, steady-state helix. It is not obvious that they should be the same as the quantities calculated from the small-amplitude theory. The amplitude dependence might be examined experimentally by using pulsed magnetic fields.

APPROACH TO EQUILIBRIUM IN QUANTUM SYSTEMS

P. Résibois*

Free University, Brussels, Belgium

(Received October 3, 1960)

In recent years, Prigogine and his co-workers have developed a general theory of approach to equilibrium in classical mechanics, using a perturbation technique on the Liouville equation.[1-3] We want to indicate here how it is possible to get similar results in quantum systems, using a representation for the density matrix, introduced first by Prigogine and Ono,[4] which stresses the formal analogy between the von Neumann equation and the classical Liouville equation. This representation has already been used in the particular cases of weakly coupled systems[4,5] and of quantum plasmas.[6]

We shall consider the case of a Fermi gas, but the method is quite general and can be applied to boson-boson or boson-fermion interactions. The Hamiltonian of the system is

$$H = H_0 + \lambda V, \tag{1}$$

$$H_0 = \sum_k \epsilon_k a_k^\dagger a_k, \tag{2}$$

$$V = \frac{1}{2\Omega} \sum_{klpr} v(klpr) a_k^\dagger a_l^\dagger a_p a_r \delta(k+l-p-r), \tag{3}$$

$$[a_k, a_{k'}^\dagger]_+ = \delta_{kk'}; \quad [a_k, a_{k'}]_+ = [a_k^\dagger, a_{k'}^\dagger]_+ = 0. \tag{4}$$

In the representation of the occupation numbers $|n\rangle$:

$$H_0|n\rangle = \sum_k \epsilon_k n_k |n\rangle \equiv \epsilon n |n\rangle, \tag{5}$$

with

$$|\mathrm{n}\rangle = |n_{k_1}, n_{k_2} \cdots\rangle. \tag{6}$$

The von Neumann equation for the density matrix ρ is ($\hbar = 1$)

$$\frac{i\partial\langle \mathrm{n}|\rho|\mathrm{n}'\rangle}{\partial t} = \lambda \sum_{\mathrm{n}''} [\langle \mathrm{n}|H|\mathrm{n}''\rangle\langle \mathrm{n}''|\rho|\mathrm{n}\rangle - \langle \mathrm{n}|\rho|\mathrm{n}''\rangle\langle \mathrm{n}''|H|\mathrm{n}'\rangle]. \tag{7}$$

We use the following notation for the matrix element of any operator A:

$$\langle \mathrm{n}|A|\mathrm{n}'\rangle \equiv A_{\mathrm{n}-\mathrm{n}'}\left(\frac{\mathrm{n}+\mathrm{n}'}{2}\right), \tag{8}$$

and we set

$$\mathrm{n} - \mathrm{n}' = \nu, \quad (\mathrm{n}+\mathrm{n}')/2 = \mathrm{N}. \tag{9}$$

It is then easy to verify that Eq. (7) can be written as

$$\frac{i\partial\rho_\nu(\mathrm{N}, t)}{\partial t} = \lambda \sum_{\nu'} \langle \nu|\delta H(\mathrm{N})|\nu'\rangle \rho_{\nu'}(\mathrm{N}, t), \tag{10}$$

where $\langle \nu|\delta H(\mathrm{N})|\nu'\rangle$ is an operator in N space defined by [see (8)]

$$\langle \nu|\delta H(\mathrm{N})|\nu'\rangle = \eta^{+\nu'} H_{\nu-\nu'}(\mathrm{N})\eta^{-\nu} - \eta^{-\nu'} H_{\nu-\nu'}(\mathrm{N})\eta^{+\nu}. \tag{11}$$

In Eq. (11) we have introduced a displacement operator such that, for an arbitrary function of N,

$$\eta^{\nu_k} f(N_k) = f(N_k + \tfrac{1}{2}\nu_k). \tag{12}$$

The formal analogy of (10) with the Liouville equation written in Fourier space is striking (see reference 1):

$$\frac{i\partial\rho_{\mathrm{k}}(\mathrm{v}, t)}{\partial t} = \lambda \sum_{\mathrm{k}'} \langle \mathrm{k}|L(\mathrm{v})|\mathrm{k}'\rangle \rho_{\mathrm{k}'}(\mathrm{v}, t). \tag{13}$$

As a matter of fact, most of the theorems on the asymptotic behavior of the formal solution of (10) in the limits

$$N \to \infty, \quad \Omega \to \infty, \quad N/\Omega = \epsilon = \text{finite}, \quad t \to \infty, \tag{14}$$

are almost identical to their classical analog.[1-3] Moreover, it can be shown that the coefficients ν describe, in complete analogy with the indexes k, the spatial correlations of the system; the perturbation operator $\langle \nu|\delta W|\nu'\rangle$, defined by (11) with V replacing H, describes the modifications of the state of correlation of the system due to the interactions.

The selection rules on $\langle \mathrm{n}|V|\mathrm{n}'\rangle$ impose similar restrictions on $\langle \nu|\delta W|\nu'\rangle$. It turns out that the nonvanishing matrix elements of the perturbation are of the same type as in classical mechanics, and we are thus led to use a diagram technique which is quite parallel to its classical analog.[1-3] However, it would be out of place to develop this diagram technique here (see also reference 5) and we shall only give the final results of the calculations.

It is possible to prove the following set of equations:

$$\frac{\partial\rho_0(\mathrm{N}, t)}{\partial t} = \sum_{n=1}^{\infty} \left\langle 0\middle|\delta W\left[\frac{-1}{\delta H_0 - i\alpha}\delta W\right]^n_{\mathrm{irr}}\middle|0\right\rangle \rho_0(\mathrm{N}, t), \tag{15}$$

$$\rho_\nu(\mathrm{N}, t) = \rho_\nu'(\mathrm{N}, t) + \rho_\nu''(\mathrm{N}, t), \tag{16}$$

$$\frac{\partial\rho_\nu'(\mathrm{N}, t)}{\partial t} + \nu\cdot\epsilon\rho_\nu'(\mathrm{N}, t) = \sum_{n=1}^{\infty} \left\langle \nu\middle|\delta W\left[\frac{-1}{\delta H_0 - i\alpha}\delta W\right]^n_{\mathrm{irr}}\middle|\nu'\right\rangle \rho_{\nu'}'(\mathrm{N}, t), \tag{17}$$

$$\rho_\nu''(\mathrm{N}, t) = \sum_{\nu'<\nu} \int_0^t dt' \langle \nu|[\exp -[i\delta H(t-t')]\delta W]_{\mathrm{creat}}|\nu'\rangle \rho_{\nu'}'(\mathrm{N}, t'), \tag{18}$$

where the notation "irr" is a symbol for the sum of all possible diagonal irreducible transitions such that no intermediate state corresponds to the correlation number ν of the initial and final state and "creat" schematizes the sum of all contributions bringing the system from a state ν' (including 0) to the state of higher correlation ν, without any intermediate state identical to ν' (irreducible creation contributions).

Here again, we have a remarkable analogy with the classical case; the nondiagonal matrix elements ρ_ν are split into two parts: ρ_ν' which describes the decay of the correlations present in the system at the initial time and ρ_ν'' which is related to lower-order correlations by creation fragments.

These equations are valid under the following assumptions:

(1) The relaxation time of the system is much larger than the duration of a collision.

(2) At the initial time $t=0$, the density matrix $\rho_\nu(\mathrm{N})$ is such that the distinction between intensive and extensive properties is already realized (see reference 1 for more details) and it describes correlations of molecular origin.

Let us also note that in the low-coupling approximation (Born approximation) we recover immediately the Pauli equations[7] and that the case of quantum plasmas has already been worked out by Balescu.[6]

It is rather straightforward to prove that, in the limit of long times, all the thermodynamical properties of the system approach the correct equilibrium value, as would be calculated with the canonical distribution $\exp(-\beta H)$. The proof of this generalized H theorem involves two stages:

(1) We first prove that the asymptotic behavior of ρ_ν' is such that

$$\rho_\nu'(\mathrm{N},t)\to 0 \text{ for } t\to\infty \quad (\nu\neq 0). \tag{19}$$

In the same limit, Eq. (17) becomes

$$\rho_\nu(\mathrm{N},t)\equiv\rho_\nu''(\mathrm{N},t)$$

$$=\sum_{n=1}^{\infty}\left\langle\nu\left|\left[\frac{-1}{\delta H_0-i\alpha}\delta W\right]^n_{\text{creat}}\right|0\right\rangle\rho_0(\mathrm{N},t). \tag{20}$$

(2) The second part of the theorem is based on the statement that if we assume that in the absence of interactions the equilibrium distribution is given by

$$\rho^0\sim\exp(-\beta H_0), \tag{21}$$

then the complete canonical distribution $\rho^{\mathrm{eq}}\sim\exp(-\beta H)$ is determined (apart from the normalization) by

$$[H,\rho^{\mathrm{eq}}]=0, \quad \rho^{\mathrm{eq}}\to\rho^0 \text{ when } \lambda\to 0. \tag{22}$$

Using the representation defined by (7) and (8), and going from the differential equation plus boundary conditions (20) to an integral equation, we can show that the equilibrium density matrix obeys

$$\rho_\nu^{\mathrm{eq}}=\rho_\nu^0\delta_{\nu,0}$$

$$-\frac{1}{\nu\cdot\epsilon-i\alpha}\sum_{\nu'}\langle\nu|\delta W(\mathrm{N})|\nu'\rangle\rho_{\nu'}^{\mathrm{eq}}(\mathrm{N}). \tag{23}$$

It is then quite easy to verify that the stationary solution of (15) and (20) indeed satisfies Eq. (23). Moreover, the expansion of (23) can be proved to be identical to the usual expansion of the Bloch equation (in temperature-integrated form).

In conclusion, we should like to stress the rather remarkable character of this Liouville-von Neumann formalism. Indeed, it allows one to treat both equilibrium and nonequilibrium problems, in classical and in quantum mechanics, by very similar techniques. This great unity is one of the most striking features of this method.

The details of the calculations, with a full description of the diagram technique we have used, will be published soon.

We wish to express our profound gratitude to Professor I. Prigogine for suggesting this work and for his constant interest during its realization. We also acknowledge fruitful discussion with Dr. R. Balescu.

---

*Aspirant au Fonds National de la Recherche Scientifique de Belgique.

[1]I. Prigogine and R. Balescu, Physica 25, 281, 302 (1959); 26, 145 (1960).

[2]I. Prigogine and F. Henin, J. Math. Phys. (to be published).

[3]F. Henin, P. Résibois, and F. Andrews, J. Math. Phys. (to be published).

[4]I. Prigogine and S. Ono, Physica 25, 171 (1959).

[5]I. Prigogine and P. Résibois, Superfluidité et équation de transport quantique (Institut Interuniversitaire des Sciences Nucléaires, Bruxelles, Belgium, 1959).

[6]R. Balescu, Physica (to be published).

[7]L. Van Hove, Physica 21, 517 (1955).

DIFFUSION OF PARTICLES IN THE EARTH'S RADIATION BELTS

N. Herlofson
Royal Institute of Technology, Stockholm, Sweden
(Received June 24, 1960; revised manuscript received October 13, 1960)

There is evidence that the outer radiation belt of the earth is fed by particles of solar or interplanetary origin, and shows great variations during geomagnetic disturbances.[1] Magnetic measurements in space vehicles indicate considerable fluctuations in the geomagnetic field within the radiation belts,[2,3] although data are not yet available on microstructures comparable to the gyration radii of electrons.

It is a reasonable conclusion that particles trapped in this fluctuating field diffuse away from the region where they are injected, and it is possible that they are accelerated by small-scale time fluctuations in the geomagnetic field in combination with scattering. Such processes are probably important in the outer radiation belt—they may even play a part in the inner belt, judging from the remarkable similarity between the particle momentum spectrum there and the general cosmic-ray spectrum.[4]

In the present note, observations[5] of the particle density near the equatorial plane at different distances from the earth will be compared with a theoretical study of the diffusion of charged particles injected into the geomagnetic field well beyond the outer radiation belt and subsequently scattered by fluctuating electric or magnetic fields.

If a particle with charge e esu, gyrating in a magnetic field H, receives an impulse Δp in a random direction normal to the magnetic field, its gyration center will be displaced by $l = c\Delta p/eH$ in a random direction normal to H,[6] provided Δp is applied during a time interval T short compared with the gyration period $2\pi mc/eH$. The random walk of a gyration center, which results from $1/T$ such impulses per unit time, corresponds to a diffusion coefficient $D = l^2/4T$ for the dispersal of the gyration centers. Writing $\Delta p = FT$, where F is an equivalent force, and choosing as an upper limit $T \leqq \pi mc/eH$, we find $D \leqq \pi c^3 m F^2/4e^3H^3$. If the disturbance force F is due to magnetic field strength variations ΔH over volumes of the order of the gyration radius, and the kinetic energy of the circular motion is 2/3 of the particle energy on the average, we find

$$D \leqq \frac{\pi c}{900}\left(\frac{\Delta H}{H}\right)^2 \frac{V}{H}, \qquad (1)$$

where V is the particle energy in electron volts, c is the velocity of light, and H is measured in gauss.

Near the equatorial plane H varies with distance r from the earth's center as r^{-3}, thus making D proportional to r^9. It is reasonable to assume that the magnetic fluctuations ΔH will either be constant or increase somewhat with distance. Regarding V, it is difficult to judge how the particle energy will vary with r. If soft particles are injected outside the outer belt, at distances corresponding to the magnetic field lines from the auroral zone, it is necessary to assume that the subsequent diffusion is accompanied by an acceleration in the fluctuating geomagnetic field, in order to account for the particle energies observed within the radiation belts.

Taking these factors into account, we adopt a diffusion coefficient proportional to r^n, where the exponent n will have to be determined from observations. n is certainly greater than 2 (which is important for the following mathematical analysis), and may possibly range up to 10 or more. When trapped particles oscillate in the earth's dipole field, diffusion across the magnetic field will then be most efficient near the equatorial plane.

For a first survey of this diffusion process it is sufficient to consider a system with spherical symmetry, where particles are injected uniformly over a spherical shell with radius a, and the diffusion coefficient $D_a(r/a)^n$ varies strongly with distance (n certainly >2).

Calling the particle density $f(r, t)$, the diffusion equation is

$$\frac{\partial f}{\partial r} = \frac{1}{r^2}\frac{\partial}{\partial r}\left[r^2 D_a\left(\frac{r}{a}\right)^n \frac{\partial f}{\partial r}\right],$$

with initial conditions at $t = 0$:

$$f(r, 0) = 0 \quad \text{for} \quad r \neq a$$
$$= \infty \quad \text{for} \quad r = a;$$
$$\int_0^\infty 4\pi r^2 f dr = 1.$$

The solution, which can be verified by substitution, is[7]

$$f(r, t) = \frac{n-2}{4\pi a^3}\frac{u^\nu}{\tau}\exp\left(-\frac{1+u^2}{\tau}\right) I_\nu\left(\frac{2u}{\tau}\right), \qquad (2)$$

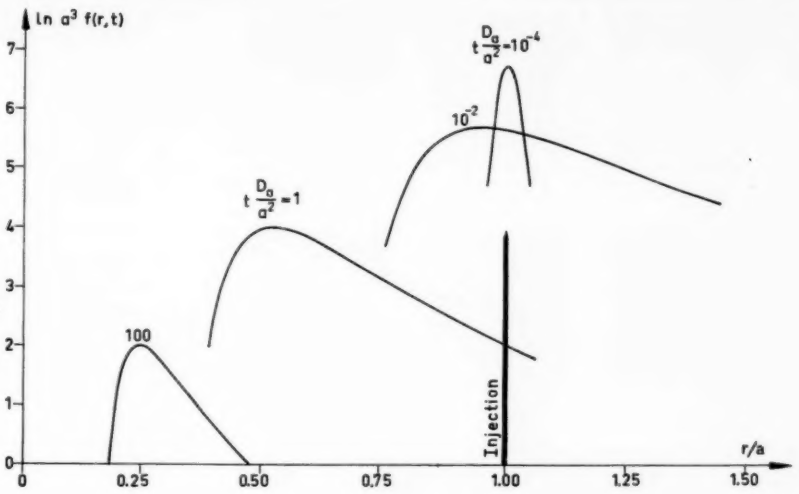

FIG. 1. Radial variation of particle density $f(r,t)$ at different times t, following the initial injection of a thin, spherical distribution at radius $r=a$ and subsequent diffusion with a diffusion coefficient proportional to r^8.

where I_ν is a Bessel function of purely imaginary argument, and the dimensionless variables are

$$u=(a/r)^{\frac{1}{2}n-1}, \quad \tau=(n-2)^2 tD_a/a^2,$$

$$\nu=(n+1)/(n-2). \tag{3}$$

The right-hand side of Eq. (2) can readily be tabulated for $n=\infty$, 8, 5, 4, $3\frac{1}{2}$, etc., corresponding to $\nu=1$, 3/2, 2, 5/2, 3, etc.

With $n=8$, Fig. 1 shows $\ln(a^3 f)$ as a function of r/a, at various times t expressed in terms of the natural time unit a^2/D_a. Immediately following the injection, a Gaussian distribution develops in the close vicinity of $r=a$, where the variations of the diffusion coefficient with distance are still insignificant. As the distribution widens, the particles closer to the earth are impeded by the diminishing diffusion coefficient, while the particles further away are rapidly dispersed. An asymmetric distribution develops with a steep slope facing the earth and a more gradual decrease outwards.

When the asymmetry is well developed, it can be shown that the peak density $f_{\max} \propto t^{-1}$ and is found at a distance $r_{\max}$ given by

$$(r_{\max}/a) \approx [(n+1)(n-2)(tD_a/a^2)]^{-n+2}.$$

In Fig. 2, observations[5] with Pioneer IV on March 3, 1959 are compared with distribution curves drawn for $n=8$ and $(tD_a/a^2)=1$ (outer belt) and 100 (inner belt). This agreement, combined with the properties of the energy spectrum in the inner belt,[4] is good enough to warrant serious consideration of combined electromagnetic acceleration and diffusion as an important process in the radiation belts.

By way of numerical illustration, we adopt $t=1$ day (10^5 sec) for the outer curve and $t=100$ days for the inner in Fig. 2. If 10-kev particles are injected at $a=43\,000$ km and scattered against magnetic irregularities, the upper limit on the diffusion coefficient in Eq. (1) then shows that the magnetic field fluctuations over the range of a gyro circle at 6-7 earth radii must be a substan-

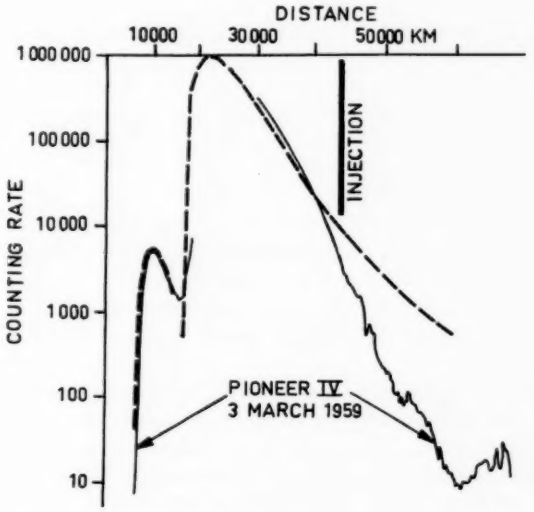

FIG. 2. Comparison between counting rates measured at different distances from the earth by the space probe Pioneer IV, and distribution curves resulting from assumed injections of particles at a distance of 43 000 km followed by diffusion with a coefficient proportional to r^8.

tial fraction (1/3-1/2) of the dipole field ($\approx 10^{-3}$ gauss) at that distance.

[1]R. L. Arnoldy, R. A. Hoffman, and J. R. Winckler, J. Geophys. Research 65, 1361 (1960).
[2]C. P. Sonett, D. L. Judge, J. M. Sims, and A. R. Kelso, J. Geophys. Research 65, 55 (1960).
[3]V. I. Krassovsky, Astronaut. Acta 6, 32 (1960).
[4]H. Alfvén, Phys. Rev. Letters 3, 459 (1959).
[5]J. A. Van Allen and L. A. Frank, State University of Iowa, August, 1959 (unpublished).
[6]H. Alfvén, Cosmical Electrodynamics (Oxford University Press, New York, 1950), Sec. 2.2.
[7]N. Herlofson, Arkiv Fysik (to be published).

INSTABILITY MECHANISMS IN TRANSVERSE PINCHES

Vernal Josephson
Space Technology Laboratories, Los Angeles, California
(Received October 10, 1960)

Neutrons have been produced in many transverse pinch assemblies when a magnetic field antiparallel to the external B_z pinching field exists in a deuterium plasma. This situation can be realized by application of a bias B_z field prior to the main driving field or is automatically realized during the second half-cycle of the oscillatory discharge since some of the first half-cycle field remains diffused in the plasma. Recent investigations on a transverse pinch assembly[1] (without mirrors) driven by a 0.14-ohm 10-μsec transmission line charged to 18 kv have revealed the presence of this trapped field and its sudden cancellation during the second compression cycle. Internal and external (fringing field) magnetic probes, Kerr cell photographs, and smear camera photographs have furnished data which allow a logical explanation of the mechanism and its importance in neutron production.

Briefly, the mechanism is as follows: The application of a fast-rising B_z field around a plasma cloud containing an internal antiparallel B_z field will cause the internal magnetic field lines to form long closed loops threading a plasma cylinder. This plasma cylinder deforms rapidly to a doughnut with surface currents flowing peripherally to maintain the accompanying closed magnetic field configuration. This configuration is identical to the Perhapsatron type of pinch and is subject to the same $m = 0$ instability which has produced neutrons in both linear and toroidal pinches.

The rate of growth of this $m = 0$ (sausage) instability and the sharpness of the interruption of the ring current supporting the trapped field will determine the energy to which the deuterons are accelerated and the consequent neutron yield. This growth rate is dependent on the plasma density and the dB_z/dt of the transverse pinch, —i.e., for low-density plasmas and large dB_z/dt, the growth will be rapid and the field cancellation violent, while for high-plasma densities, the trapped magnetic field can be maintained for much longer times. Ions in this configuration, accelerated by this mechanism, will continue to orbit in the uniform field until they drift out of the ends or collide with other particles. Thus, neutron generation can begin

(a) Transverse Smear

(b) Axial Smear

FIG. 1. Transverse and axial smear photographs showing the plasma-trapping mechanism.

with the sudden field cancellation and continue as long as the magnetic field maintains stable-orbit conditions.

Figure 1 shows smear photographs taken at 100μ D_2 pressure monitoring (a) radial behavior of the plasma at the end of the drive solenoid, and (b) the axial behavior of the plasma (observing from the solenoid center to 8 cm outside). During the first 10-μsec compression cycle of the pre-ionized, field-free plasma, absence of trapping is indicated by the luminous radial oscillations outside of the solenoid, and by the high-velocity axial jetting. During the second 10-μsec compression cycle when there is a reverse internal field remaining from the first compression cycle, trapping is indicated by the absence of luminosity outside of the solenoid, and the plasma cylinder-to-doughnut deformation is indicated by axial motion of the luminosity towards the solenoid center. Following the trapped-field cancellation, the luminosity again moves axially out of the solenoid. The phenomenon is quite reproducible if pressure and B_z conditions are kept constant.

Figure 2 shows a series of Kerr cell photographs depicting the growth and blowup of the instability mechanism, and the times of viewing. Accompanying these are typical fringing B_z waveforms for the vacuum case and the plasma and trapped field case, and the internal B_z waveforms for a plasma case. The trapped field is indicated in the internal B_z-plasma case by the nonreversal in the 10-15 μsec interval and also in the fringe B_z-plasma case by the decrease in magnetic field strength during the trapping interval. However, the Kerr cell photographs were obtained when no internal probes were in the system, and they are strongly indicative of breakup of the plasma doughnut into irregular sausages which one would expect with the growth of the $m=0$ instability.

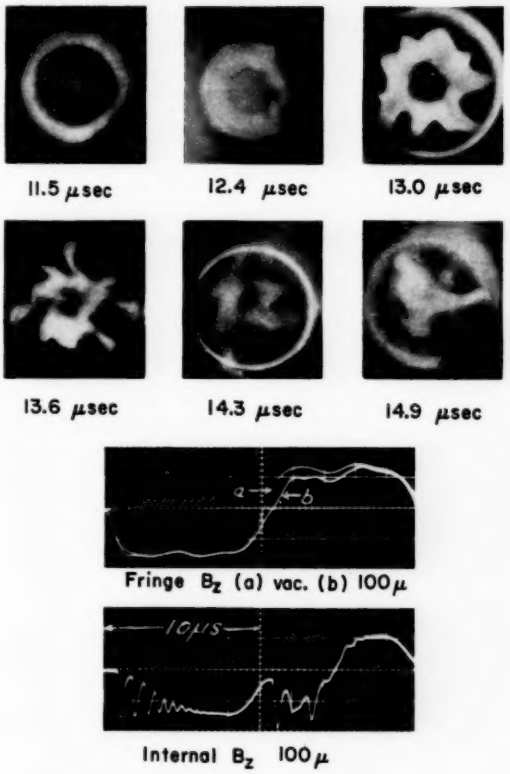

FIG. 2. Kerr cell photographs and internal B_z and fringe B_z waveforms depicting the formation and growth of the instability mechanism.

[1]M. Dazey, V. Josephson, and R. Wuerker, Bull. Am. Phys. Soc. 5, 340 (1960).

EVIDENCE FOR THE SOLAR CORPUSCULAR ORIGIN OF THE DECAMETER-WAVELENGTH RADIATION FROM JUPITER*

Thomas D. Carr and Alex G. Smith
Department of Physics, University of Florida, Gainesville, Florida

and

Heins Bollhagen,
Maipú Radioastronomical Observatory, University of Chile, Santiago, Chile
(Received August 22, 1960; revised manuscript received October 3, 1960)

Various speculations have been made regarding the origin of the intense but sporadic radiation emitted by Jupiter at decameter wavelengths. Discharges of atmospheric electricity,[1] volcanic explosions,[2] atmospheric chemical reactions,[3] and charged particles arriving from the sun[4] have all been suggested as possible sources of the energy. Dr. Eugene Epstein of Harvard College Observatory pointed out to the writers that if solar particles are the cause, one would expect the radio emissions to be correlated with geomagnetic activity at the time of Jovian opposition. A search for such a correlation was made by the writers during the recent opposition. An apparent correlation was found to exist.

The radio observations were made at the Maipú Radioastronomical Observatory near Santiago, Chile. The observations used in the present analysis extended from April 29, 1960, to August 3, 1960. Opposition occurred on June 20, 1960. The frequencies employed were 18 Mc/sec until May 30, and both 18 Mc/sec and 10 Mc/sec after May 30. The antennas were dipole arrays providing about 6 hours of Jupiter coverage each night. Commercial receivers and low-speed pen recorders were used. Geomagnetic and solar data were obtained from the High Altitude Observatory, Boulder, Colorado.

The daily Jupiter activity index is plotted as a function of date in the upper part of Fig. 1. The Jupiter activity index for a given date is defined as the mean height of the three largest noise pulses (corrected for any variations in gain) multiplied by the duration of the activity, divided by the duration of the observation period. The geomagnetic *A* index is plotted as a function of date in the lower part of Fig. 1. The histograms have been so displaced that the dates on the lower one match dates 9 days later on the upper one. Some degree of correlation between the two histograms is apparent.

The letters on the lower histogram indicate the starting times of all geomagnetic storms reported during the period. Capitals indicate storms for which the associated solar flare had been observed earlier; no associated flares were observed for the storms indicated by lower case letters. The velocities of the leading particles in those storms

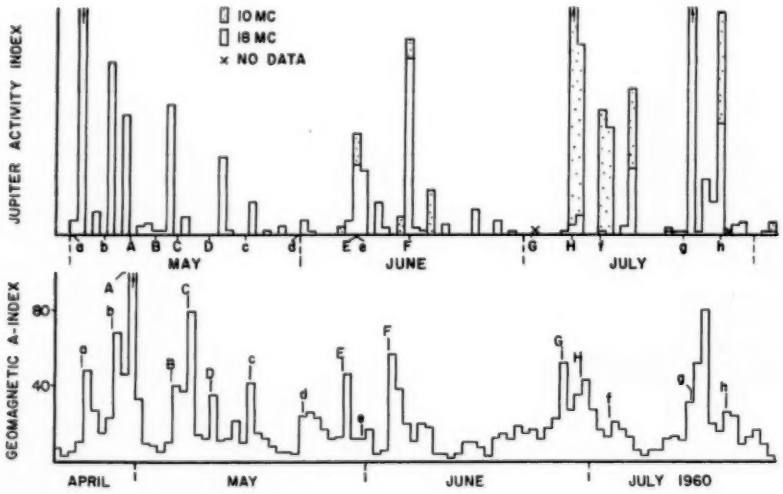

FIG. 1. Upper histogram: Jupiter activity index plotted as a function of date. Clear bars and dotted bars refer to 18 Mc/sec and 10 Mc/sec reception, respectively. Dates for which data were not available are indicated by ×. Lower histogram: Geomagnetic *A* index plotted as a function of date. All dates are Universal Time.

designated by capitals could be calculated, since their times of departure from the sun and arrival at the earth had been observed. The arrival times at Jupiter were determined for these particles; they are indicated by capitals on the upper histogram. Approximate arrival times for the leading particles in the storms not preceded by observed flares are determined by assuming that the travel time from the earth to Jupiter is 8 days. This is approximately the average time for those particles of known velocity to travel the same distance.

There seems to be a pronounced correlation between the arrival dates of storm particles at Jupiter and the dates of occurrence of major Jupiter noise storms. In most instances the indicated arrival dates and the days of greatest Jupiter activity coincide or are separated by only a day or two.

Data on the events identified by capitals are given in Table I. The angular distance of a flare from the center of the sun's disk as viewed from Jupiter is designated by α. For the events in Table I, one would expect the best correlation with Jupiter activity for small values of α and for times close to opposition. Most of the events identified by lower case letters were due to the passage of solar M regions. For these events, correlation with Jupiter activity should not be limited to the time of opposition, although deviations of at least a day or two in the actual arrival times from the indicated values are to be expected. It should be noted that the correlation would not have been as good if only the 18 Mc/sec data had been used. Some intense noise storms occurring at the lower frequencies are not detected at 18 Mc/sec (although very few are entirely confined to frequencies above 18 Mc/sec). It is believed that the correlation would be better if there were wider frequency coverage and 24-hour-per-day time coverage (from a world-wide chain of observatories).

The results presented in Fig. 1 seem to indicate that the radiation from Jupiter at decameter wavelengths is caused by the influx of charged particles from the sun. A theory of the radiation based on this conclusion must account for at least two other well-established phenomena, namely, the concentration of the noise sources into one or more relatively narrow longitude zones which maintain the same rotational period for at least several years, and the great predominance of radiation which is right-handed elliptically polarized.[5] To account for the longitude effect, the writers propose that there are one or more magnetic poles (or other field anomalies) near the surface of the planet which are some distance from the geographical poles. The charged solar particles tend to spiral into the magnetic poles, causing a local increase in particle concentration. Whatever the actual radiative process is, more radiation would be expected from such regions, and the source areas would thus rotate with the period of the solid crust of the planet.

If Jupiter's magnetic field is a dipole field, then it must be assumed that the dipole axis and the rotational axis do not coincide. Since observations do not indicate two equal noise source areas 180° apart in longitude, the additional assumption must be made that the dipole center does not coincide with the center of the planet. However, another possibility is that the radiation is emitted by electrons in the vicinity of anomalies in the

Table I. Data on flares and associated particles.

Event identification	Date	Flare Importance number	Particle travel time Sun to Earth	Earth to Jupiter	α (degrees)
A	April 28	3	48.0 hr	9 days 4 hr	83
B	May 4	2	33.7 hr	6 days 8 hr	53
C	May 6	3+	38.3 hr	7 days 4 hr	58
D	May 9	3	45.6 hr	8 days 11 hr	92
E	May 26	2+	59.2 hr	10 days 12 hr	4
F	June 1	3+	66.5 hr	11 days 17 hr	56
G	June 25	3	29.0 hr	5 days 1 hr	18
H	June 27	3	45.9 hr	8 days	45

intense dipole field which has been postulated by Field[6] to account for the decimeter (microwave) radiation from Jupiter. In this case the dipole axis and rotational axis are assumed to coincide, the rotation of the field anomalies causing the observed periodicity. Both the decameter and the decimeter radiation could thus be due to cyclotron emission if this model is assumed.

The observations which have been described cannot be repeated until the period from about June through August, 1961, when the earth will again pass between the sun and Jupiter. Observing conditions at this time will be best in the southern hemisphere, since severe interference from summer thunderstorms will be experienced in the northern hemisphere.

The writers are greatly indebted to Dr. Federico Rutllant, director of the National Astronomical Observatory and the Maipú Radioastronomical Observatory of the University of Chile, without whose assistance the Chilean observations would have been impossible.

---

*This program has been supported by the National Science Foundation, the U. S. Army Office of Ordnance Research, and the Office of Naval Research.

[1]Nature 175, 1074 (1955).

[2]R. M. Gallet, Report of the Union Radio-Scientifique Internationale - U. S. National Committee, Twelfth General Assembly, National Academy of Sciences - National Research Council Publication No. 581 (1958), p. 143.

[3]C. Sagan, report to American Astronomical Society meeting, Mexico City, 1960 (unpublished).

[4]T. D. Carr, report to American Astronomical Society meeting, Gainesville, Florida, 1958 (unpublished).

[5]A. G. Smith and T. D. Carr, Astrophys. J. 130, 641 (1959).

[6]G. B. Field, J. Geophys. Research 65, 1661 (1960).

MAGNETIC SUSCEPTIBILITY OF THE TWO PHASES OF LITHIUM AT LOW TEMPERATURES

F. T. Hedgcock
Department of Physics, University of Ottawa, Ottawa, Canada
(Received August 26, 1960; revised manuscript received October 4, 1960)

Since the initial discovery of a phase transformation in lithium,[1] experimental studies of the influence of the transformation on various physical properties have been undertaken.[2-4] Some of these measurements[3] can be interpreted on the basis of a change in the equilibrium electron properties when transforming from the bcc to the low-temperature hcp phase. To be specific, the resistance results can be interpreted as due to a change of approximately 20% in the density of states on transforming lithium to the hcp phase. Since the magnetic susceptibility may be considered to consist of the sum of the susceptibility of the lithium ions and the susceptibility of the conduction electrons, a density-of-states change should be observable as a change in the total susceptibility of lithium. Preliminary results have been reported on the susceptibility of lithium at low temperatures[5] but considerable doubt existed as to whether the observed change in the susceptibility was actually related to the phase transformation. Present difficulties in the interpretation of measurements on the susceptibility of lithium involve apparent changes in the ferromagnetic corrections on temperature cycling of the sample. However, owing to the considerable interest in the properties of lithium and since specific heat measurements at present yield no information about electronic changes associated with the low-temperature phase transformation, more recent measurements on the susceptibility of lithium in the temperature region 115°K-60°K where the transformation takes place have been made and are reported here.

The samples of lithium used in these measurements were of the highest purity available and were supplied by the Lithium Corporation of America.[6] The Curie method was used to determine the susceptibility of the lithium samples which were in the form of bare rods. The amount of ferrous impurity present in precipitated form would correspond to two parts per million of iron if a saturation value of 200 emu/g is assumed for the saturation magnetic moment. The absolute room temperature susceptibilities of the samples used range from $(1.89 \pm 0.01) \times 10^{-6}$ to $(1.93 \pm 0.01) \times 10^{-6}$ emu/g and are in reasonable agreement with the value reported by Pugh and Goldman.[7] Investigations of the temperature

dependence of the susceptibility of lithium above the region of the phase transformation (150°K-300°K) showed a very slight T^{-1} paramagnetism which indicates paramagnetic impurities in solution. The influence of oxygen on the susceptibility of the alkali metals has already been emphasized.[8]

Table I contains susceptibility measurements on various samples. In order to eliminate the contribution due to dissolved paramagnetic impurities the susceptibilities of sample 7 were all measured at 80°K before and after transforming the sample at 60°K. When the above procedure was not followed a paramagnetic correction

Table I. Magnetic susceptibility of lithium sample 7 and force on lithium samples 3, 4, and 5 as a function of temperature. The maximum average magnetic field applied to all samples was 5.6 koe. (We use K to denote volume susceptibility, to distinguish it from the mass susceptibility χ.)

T(°K)	$K(H_{max})$ (6.85-4.28 koe)[a] (emu/cm^3)	Force (arbitrary units)
	Sample 7	
115	0.196×10^{-6}	
80	0.207×10^{-6}	
60(80)	0.226×10^{-6}	
115	0.202×10^{-6}	
80	0.224×10^{-6}	
60(80)	0.236×10^{-6}	
After annealing at room temperature for 15 hours		
115	0.224×10^{-6}	
80	0.236×10^{-6}	
60(80)	0.254×10^{-6}	
115	0.237×10^{-6}	
80	0.237×10^{-6}	
60(80)	0.255×10^{-6}	
115	0.238×10^{-6}	
	Sample 5	
115		8.05
80		8.10
75(80)		8.32
65(80)		8.52
	Sample 4	
73		9.79
62		9.16
53		9.34
93		8.71
	Sample 3	
120		9.42
60(90)		9.90
120		9.42

[a]Probable error in K values is $\pm0.002\times10^{-6}$ emu/cm^3.

was applied (see sample 4). It can be seen that the value of the susceptibility does not recover after the sample has received a low-temperature cycling and that there is a residual effect due to the phase transformation. After lithium sample 7 had been twice cycled, the susceptibilities at the various temperatures were reproducible. Dividing the susceptibility hysteresis into two parts, the hysteresis which is not associated with the phase transformation is presumably a result of changes in the contribution due to ferrous impurity. To investigate this effect, the room temperature susceptibility was measured before and after quenching at 4.2°K. These results are shown in Fig. 1 for a sample containing appreciable ferrous impurity. It will be noticed that the ferromagnetic component is decreased and the apparent susceptibility value of lithium is increased as a result of the quench. The observed effect is probably due to straining the incoherently precipitated ferrous inclusion since cold working at room temperature resulted in a similar behavior of the ferromagnetic component and the apparent susceptibility of lithium.

Figure 2 shows the H^{-1} dependence of the sus-

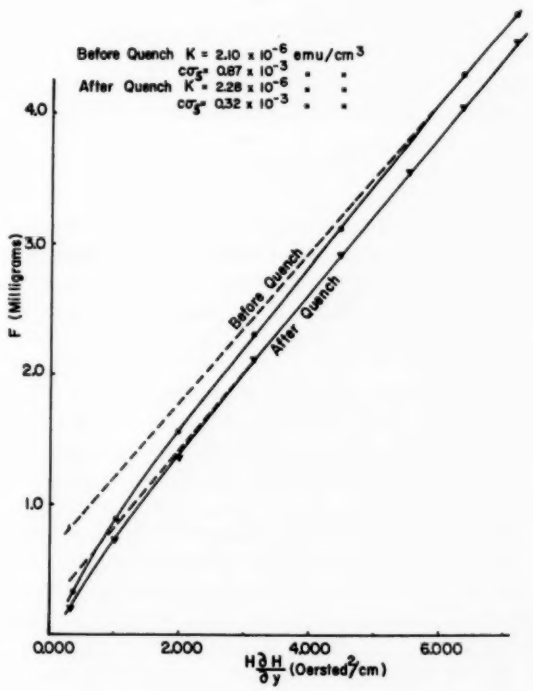

FIG. 1. Force on commercial lithium sample as a function of $H\partial H/\partial y$ before and after quenching at 4.2°K.

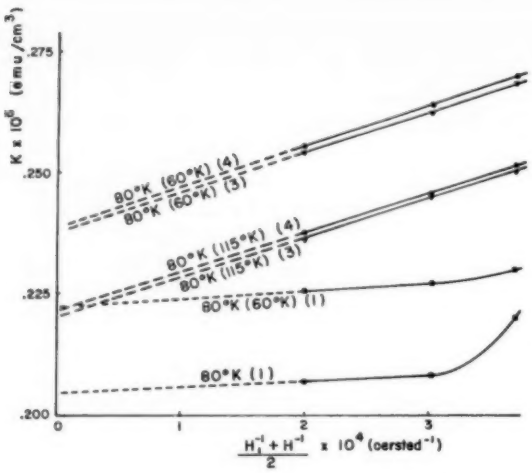

FIG. 2. Susceptibility of lithium sample No. 7 as a function of the reciprocal of the average field. The bracketed temperature is the preceding temperature of the lithium sample. The bracketed number is the number of times the sample was brought to that temperature.

ceptibility of lithium sample 7 at 80°K before and after cooling to 60°K. Provided a high enough magnetic field is applied to the susceptibility sample to reach the linear portion of the saturation curve for the ferrous impurity, the intercept of the graph in Fig. 1 yields the susceptibility of the sample at infinite magnetic field and the slope of the line is $C\sigma_S$, where C is the concentration and σ_S is the specific saturation intensity of magnetization of the ferrous impurity. Evidence that sufficiently high magnetic fields were available in the present experiments can be obtained from Fig. 1 where the linear portion of the curve for the quenched sample commences at a field strength of approximately 3000 oersteds. The slopes of the lines in Fig. 2 are equal at 80°K after warming to 115°K and at 80°K after cooling to 60°K, indicating that no change has taken place in the behavior of the ferrous impurity on cycling. The residual effect is presumably due to a change in the susceptibility on converting the lithium to the low-temperature phase and yields a value of approximately 6-7% for the susceptibility change on converting sample 7 to a 25%-75% mixture of the hcp and bcc phases (see Barrett[1]). Samples 3, 4, and 5 indicate a susceptibility change between 5 and 6% for a 25% conversion. This means that a susceptibility change of approximately 24% could be suggested in converting lithium from the bcc to hcp phase.

Assuming[9] a parabolic band and a density-of-states effective mass m^* equal to the electron effective mass averaged for motion in a magnetic field, the electronic susceptibility can be written

$$\chi_e = \frac{4\mu_0^2 m^*}{\rho h^2}(3\pi^2 n)^{1/3}[1 - \tfrac{1}{3}(m/m^*)^2].$$

Further, if the observed change in the susceptibility is interpreted as a change in χ_e, this would correspond to a 40-50% increase in m^* in converting from bcc to hcp lithium. If the hcp phase of lithium is considered to be a highly faulted fcc structure,[10] then on the Cohen and Heine[11] electronic band model this Δm^* would correspond to an increase in the band gap Δ_{sp} and the Fermi surface in lithium would then make greater contact with the zone boundary in the hcp structure than in the bcc structure.

Measurements on lithium are being continued at higher magnetic fields and attempts are currently being made to reduce the ferrous content of available lithium samples. Similar effects of quenching on χ_{ferrous} have been observed in sodium, and at present measurements on high-purity distilled sodium are being made where the experimental difficulties of preparing ferrous free samples are not as great as in the case of lithium.

The author would like to express his thanks to Dr. J. S. Dugdale for his continued interest in this work and to Dr. D. Gugan for communication of results before publication. Special thanks are due to Dr. A. Siddiqi who performed the room temperature susceptibility measurements and to Mr. G. Mark who assisted in making the low-temperature measurements.

---

[1]C. S. Barrett, Am. Mineralogist 33, 749 (1958).
[2]D. L. Martin, Proc. Roy. Soc. (London) A254, 444 (1960).
[3]J. S. Dugdale and D. Gugan (to be published).
[4]Z. S. Basinski and L. Verdini, Phil. Mag. 48, 1311 (1959).
[5]F. T. Hedgcock, Proceedings of the Fifth International Conference on Low-Temperature Physics and Chemistry, Madison, Wisconsin, August 30, 1957, edited by J. R. Dillinger (University of Wisconsin Press, Madison, 1958).
[6]A typical resistive ratio of the samples used is 2×10^{-3}.
[7]W. Pugh and J. E. Goldman, Phys. Rev. 99,

1633(E), 1641(A) (1955).
[8]F. T. Hedgcock, Can. J. Phys. 34, 1164 (1956).
[9]Some experimental justification for this approximation can be found from the fact that the density of states calculated from χ_p determined from electron spin resonance results and that found from χ_e for the bcc phase agree within the experimental error of the measurements.
[10]C. S. Barrett, Phase Transformations in Solids (John Wiley & Sons, Inc., New York, 1951), p. 354.
[11]M. H. Cohen and V. Heine, Suppl. Phil. Mag. 1, 395 (1958).

THEORY OF HOT-ELECTRON EFFECTS IN MANY-VALLEY SEMICONDUCTORS IN THE REGION OF HIGH ELECTRIC FIELD

H. G. Reik, H. Risken, and G. Finger
Philips Research Laboratories, Aachen, Germany
(Received September 26, 1960; revised manuscript received October 10, 1960)

The quantitative description of hot-electron effects in many-valley semiconductors is obtained by means of the solution of a properly formulated Boltzmann equation for high fields. A proper formulation implies that one takes into account the actual band structure and the actual scattering mechanisms (acoustical, optical, and intervalley scattering) in terms of the deformation potential theory.

To solve this equation, one defines for convenience the effective momenta $\vec{p}^*$ and the effective electric fields $\vec{F}^*$ for each valley by

$$p_x^* = p_x, \quad p_y^* = p_y, \quad p_z^* = (m_t/m_l)^{1/2} p_z;$$

$$F_x^* = F_x, \quad F_y^* = F_y; \quad F_z^* = (m_t/m_l)^{1/2} F_z,$$

where z is the longitudinal axis of the valley under consideration.

A detailed analysis of the case of n-type Ge has shown that one may write the distribution function for electrons in the valley i as

$$f^{(i)}(p^*, \theta) = f_0^{(i)}(\epsilon) + f_1^{(i)}(\epsilon) P_1(\cos\theta). \qquad (1)$$

Here ϵ is the energy of the electron, and θ is the angle between the directions of the effective field and the effective momentum.

In this note we neglect intervalley scattering and electron-electron collisions. We restrict ourselves to a range of mean energies of the electrons so that the following conditions are met: The mean energies of the electrons are much larger than $\hbar\omega_{\text{opt}}$. Momentum relaxation of the electrons is due to acoustical and optical scattering; energy relaxation is due only to optical scattering. We then find the following results:

1. $f_0^{(i)}(\epsilon)$ is a Maxwellian distribution over most of the energy range with only slight deviations for $\epsilon < 2\hbar\omega_{\text{opt}}$ and $\epsilon > 100kT_{\text{latt}}$.[1] The electron temperature

$$T_e^{(i)} = (eh^3 \rho c_l F^{*(i)})^2 / (96\pi^4 k^2 m_t^3 m_l \Xi_{\text{av}}^2 D^2 T^*), \qquad (2)$$

where

$$T^* = T_{\text{latt}} + [hc_l(2n_{q\,\text{opt}} + 1)D^2 / (4\pi k \omega_{\text{opt}} \Xi_{\text{av}}^2)],$$

is in general different for different valleys. It is proportional to the energy supplied by the electric field [$\sim(F^{*(i)})^2$] and inversely proportional to the losses in energy and momentum, which depend on the lattice temperature and the deformation potential constants.

2. The drift velocity is given by

$$v_d = hc_l DS / [\pi^{3/2}(3m_t kT^*)^{1/2} \Xi_{\text{av}}], \qquad (3)$$

and is independent of the electric field. S is a slowly varying function of the orientation of the sample. For a Sasaki type of experiment[2] [drift velocity in a (110) plane] S varies between 0.83 and 0.76.

3. The optical deformation potential constant can be evaluated from measurements of the saturation drift velocity using (3). For the evaluation a mean value of $S = 0.80$ and $\Xi_{\text{av}} = 11$ ev (calculated with $\Xi_u = 17$ ev,[3] $\Xi_d = -5.8$ ev[4]) has been used.

The result is shown in Table I. (Koenig's values of v_d are calculated from measurements of the saturation current density.)

The values of D are consistent with the analysis of mobility data by Brooks.[5] They are of the same order of magnitude as a value given by Meyer,[6] $D = 1.15 \times 10^9$ ev/cm, which was extracted from experimental data on infrared ab-

Table I. Evaluation of the optical deformation potential constant D from measurements of the saturation drift velocity v_d at different lattice temperatures.

Author	T_{latt}	v_d (cm/sec)	D (ev/cm)
Ryder[a]	77	0.9×10^7	0.37×10^9
	193	0.76×10^7	0.49×10^9
	298	0.62×10^7	0.49×10^9
Gunn[b]	300	0.55×10^7	0.43×10^9
Koenig[c]	80	1.08×10^7	0.47×10^9
	300	0.60×10^7	0.47×10^9
Koenig et al.[d] $\langle100\rangle$ sample	297	0.67×10^7	0.51×10^9

[a]E. F. Ryder, Phys. Rev. 90, 766 (1953).
[b]J. B. Gunn, J. Electron. 2, 87 (1956).
[c]S. H. Koenig, Proc. Phys. Soc. (London) 73, 959 (1959).
[d]S. H. Koenig, M. I. Nathan, W. Paul, and A. C. Smith, Phys. Rev. 118, 1217 (1960).

sorption by free carriers obtained by Fan, Spitzer, and Collins.[7]

4. The calculated anisotropy of hot electrons in a Sasaki type of experiment is shown in Fig. 1. The values of $\tan\psi$ are much higher than those calculated by Shibuya[8] but they are still too low compared with measurements of Koenig[9,10] and Schmidt-Tiedemann.[11] The deviations between this theory and the experiments can be accounted for by intervalley scattering (to be treated in a shortly forthcoming note).

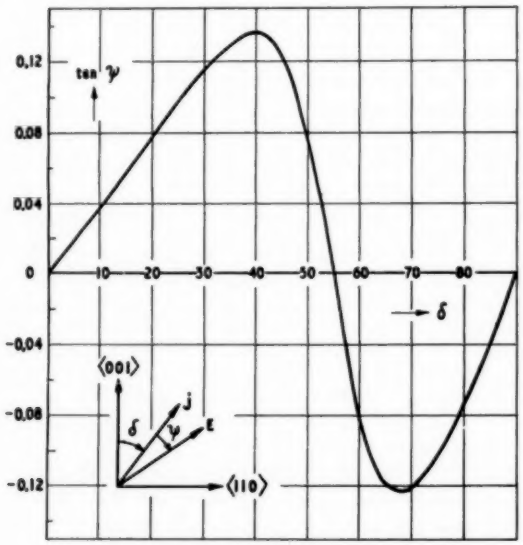

FIG. 1. Anisotropy of hot electrons.

5. In order to estimate the limits of applicability of the results, we shall now briefly outline our calculations. For mean energies of the electrons much larger than the energy of an optical phonon, we retain only optical terms in the energy relaxation and expand all optical scattering terms in the Boltzmann equation linearly in $\hbar\omega_{opt}/\epsilon$. $f_0^{(i)}$ and $f_1^{(i)}$ are then determined by the equations:

$$\epsilon df_1^{(i)}/d\epsilon + f_1^{(i)} = -\alpha_0^{(i)}(\epsilon df_0^{(i)}/d\epsilon + f_0^{(i)}), \qquad (4)$$

$$df_0^{(i)}/d\epsilon = \alpha_1^{(i)} f_1^{(i)}, \qquad (5)$$

$$\alpha_0^{(i)} = 6\pi m_t^{3/2} m_l^{1/2} D^2/(eh^2\rho F^{*(i)}),$$

$$\alpha_1^{(i)} = 16\pi^3 k m_t^{3/2} m_l^{1/2} \Xi_{av}^2 T^*/(eh^4\rho c_l^2 F^{*(i)}).$$

The usual elimination procedure leads to the Maxwellian type of $f_0^{(i)}$ with the electron temperature (2); use of (5) gives (3). The approximations made in deriving (4) and (5) are justified for electron temperatures of 1500°K and higher. The assumption that energy loss is due only to optical scattering is true for $T_{el} < 100 T_{latt}$.[1] Equation (2) gives thus a relation between effective fields and lattice temperatures, determining the range of experimental conditions for the applicability of the theory.

6. For electron temperatures below 1500°K one has to retain quadratic terms in $\hbar\omega_{opt}/\epsilon$ in the expansion of optical scattering terms in the Boltzmann equation. We then find a new Maxwellian distribution as solution for $f_0^{(i)}$ with $T_e^{(i)}$ replaced by $T_e^{(i)}[1+(\hbar\omega_{opt}/2kT_e^{(i)})(2n_{q\,opt}+1)]$.

The mean effective momentum $\bar{p}^{*(i)}$, which before was independent and equal to $\bar{p}_{sat}^{*(i)}$, now becomes field dependent:

$$\bar{p}^{*(i)} = \bar{p}_{sat}^{*(i)}\left(1 - \frac{\hbar\omega_{opt}}{4kT_e^{(i)}}(2n_{q\,opt}+1)\right).$$

The drift velocity also becomes field dependent and the anisotropy is lowered.

We thank Professor D. Polder, Dr. H. J. G. Meyer (Eindhoven), Professor W. Franz, and Dr. K. J. Schmidt-Tiedemann (Hamburg) for

helpful and stimulating discussions.

[1]E. Conwell, J. Phys. Chem. Solids 8, 234 (1959); Bull. Am. Phys. Soc. 5, 61 (1960).
[2]W. Sasaki, M. Shibuya, K. Mizuguchi, and G. M. Hatoyama, J. Phys. Chem. Solids 8, 250 (1959).
[3]C. Herring and E. Vogt, Phys. Rev. 101, 944 (1956).
[4]C. Herring, private communication to H. J. G. Meyer cited in J. Phys. Chem. Solids 8, 264 (1959).
[5]H. Brooks, Advances in Electronics, edited by L. Marton (Academic Press, New York, 1955), Vol. 7, p. 85.
[6]H. J. G. Meyer, Phys. Rev. 112, 298 (1958); J. Phys. Chem. Solids 8, 264 (1959).
[7]H. J. Fan, W. Spitzer, and R. J. Collins, Phys. Rev. 101, 566 (1956).
[8]M. Shibuya, Phys. Rev. 99, 1189 (1955).
[9]S. H. Koenig, Proc. Phys. Soc. (London) 73, 959 (1959).
[10]S. H. Koenig, M. I. Nathan, W. Paul, and A. C. Smith, Phys. Rev. 118, 1217 (1960).
[11]K. J. Schmidt-Tiedemann (private communication).

RESONANT SPIN-SPIN INTERACTION BETWEEN DONORS AND ACCEPTORS IN SILICON

R. A. Levy
Hughes Products, Newport Beach, California
(Received September 27, 1960; revised manuscript received October 11, 1960)

A reduction of the direct relaxation time of donor electrons in silicon, believed to be due to a resonant spin-spin interaction[1] with a background acceptor resonance line, has been observed in compensated silicon containing[2] approximately 5×10^{15} phosphorus donors/cm^3 and approximately 3×10^{15} boron acceptors/cm^3. Observations were made in both strained and unstrained samples after populating all the donor and acceptor states with optical radiation at liquid helium temperature.[2,3] Two effects were observed: The first was a reduction, after irradiation, of the relative amplitude of one of the donor hyperfine components with respect to the other; the second was a reduction of relative amplitude of both donor hyperfine components with respect to the amplitude before irradiation. Results were obtained by studying the decay of magnetization at the resonant mixing field using the electron spin resonance signal as a monitor.

The procedure for each run was as follows: (1) With rf power turned off, magnetize the sample at a high field (9000 oersteds) long enough to come to thermal equilibrium at this field; (2) reduce the field to H_{mix} and leave it there for a specified length of time; (3) turn on rf power and sweep through resonance to check how much the magnetization had decayed while at the mixing field. Figure 1 shows recordings of the phosphorus resonance[4] with a calibrating marker of conduction electrons added (0.5 mg of silicon containing $\approx3\times10^{18}$ P/cm^3). *a*, *b*, and *c* constitute a series of runs taken before irradiation; *d*, *e*, and *f* are a series taken after irradiation. The top row is for no time in the mixing field and is a measure of the equilibrium magnetization at 9000 oersteds. The increased donor concentration after irradiation is to be noted.

Data taken before irradiation show no difference between the two hyperfine components of the phosphorus donor resonance, and the relaxation time indicated by successive traces is in substantial agreement with previously reported[5] work on donors in silicon without compensation (~500 seconds).

Data taken after irradiation with the sample unstrained (middle row of Fig. 1) indicate that the $m_I=-1/2$ component is relaxing about 50% faster than the $m_I=+1/2$ component. According to Feher's[1] description of the resonant spin-spin interaction, this indicates an overlap with a background resonance line at the mixing field ($\approx$80 oersteds for this case). Since this type of behavior does not occur before light populates the acceptor states, it is concluded that the acceptor resonance is responsible.

Comparison with data before irradiation also indicates that the $m_I=+1/2$ component is relaxing about twice as fast as it was before, showing that the background acceptor line is broad enough to overlap both hyperfine components; however, the $m_I=-1/2$ component is closer to the center. Since the sample was under no externally applied uniaxial strain, the width of the acceptor line[6] would be expected to be quite large. As pointed out by Feher,[1] the sensitivity of this technique makes it possible to observe relatively low concentrations of species with broad resonances. In this case the observation of a line perhaps several hundred oersteds wide

resulting from the order of 10^{15} acceptors/cm^3 was possible.

The g value of the acceptor line is calculated by equating the transition energies of the acceptor and the $m_I = -1/2$ hyperfine component of the donor. For the donor, assuming $g_D = 2$, we have from the Breit-Rabi formula

$$\Delta E_D = \tfrac{1}{2}[-1 + x + (1+x^2)^{1/2}], \qquad (1)$$

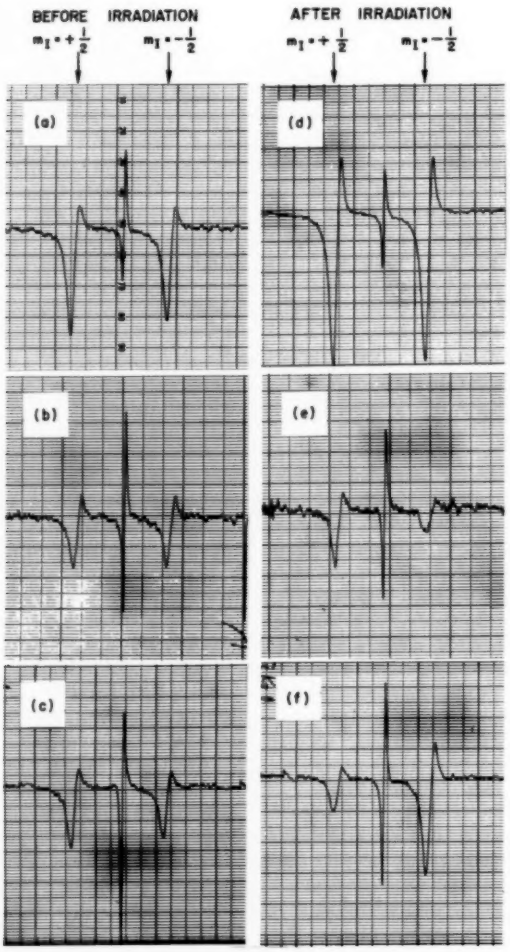

FIG. 1. Phosphorus resonance signal in compensated silicon before (left column) and after (right column) optical irradiation of sample. Top row (a and d): Sample strained or unstrained, no time spent in mixing field. Middle row (b and e): Sample unstrained, 5 minutes at $H_{mix} \approx 80$ oersteds. Bottom row (c and f): Sample strained perpendicular to direction of dc magnetic field, $3\frac{1}{2}$ minutes at $H_{mix} \approx 120$ oersteds. (Data: $T = 1.5°$K, $f_0 \approx 9000$ Mc/sec, $\approx 5\times10^{15}$ P/cm^3, $\approx 3\times10^{15}$ B/cm^3).

where $x = 2\mu_0 H/ah = H/43 \approx 1.9$ at $H_{mix} \approx 80$ oersteds for the phosphorus donor. The acceptor transition energy can be expressed by the linear relation

$$\Delta E_A = g_A x/2. \qquad (2)$$

Equating (1) and (2) and solving for g_A, we obtain

$$g_A = [-1 + x + (1+x^2)^{1/2}]/x \approx 1.6.$$

This is in fair agreement with the center of gravity of the results of Feher, Hensel, and Gere[6] since the exact center of the overlap is probably not sharply defined, and with no information about the internal strain distribution in the sample.

When the sample is subjected to a uniaxial stress of approximately 250 kg/cm^2 perpendicular to the dc magnetic field, the effect is to reverse the situation and reduce the relative amplitude of the $m_I = +1/2$ component, as is shown in the bottom row of Fig. 1 after irradiation. $H_{mix} = 120 \pm 15$ oersteds. Equating transition energies for acceptor and $m_I = +1/2$ component, we obtain

$$g_A = [1 + x + (1+x^2)^{1/2}]/x$$

$$= 2.43 \pm 0.06.$$

If the data of Feher et al.[6] for boron are extrapolated to a stress of 250 kg/cm^2, their value of g_A would be 2.39, which is within the experimental error of our results. Experiments are in progress to vary the strain direction and the acceptor and thereby allow verification of acceptor g values throughout their expected range.

Figure 2(a) shows the relative difference in amplitude $(A_+ - A_-)/A$ plotted as a function of time in the mixing field for samples with two different acceptor concentrations: A, the original sample, and B, containing $\approx 5\times10^{14}$ B/cm^3 and $\approx 5\times10^{15}$ P/cm^3. The effect is reduced several-fold in the dilute sample. Figure 2(b) shows the field dependence of the absolute magnitude of $(A_+ - A_-)/A$. Optimum H_{mix} is more sharply defined when the sample is strained, indicating a narrower acceptor line.

Measurements were made on a Varian EPR spectrometer modified to allow independent phase and amplitude bridge balance. Dispersion signals were obtained by a phase-amplitude unbalance method.[7] A half-wave TE_{101} gold-plated brass resonant cavity was slotted horizontally in the center of both narrow sides to

permit entry of light. Optical radiation was provided by two American Optical Company unfiltered microscope lamps. Samples consisted of slabs of (100)-oriented silicon of dimensions $0.370\times0.760\times0.040$ inch. Stress was applied by compressing the sample between Teflon slabs during assembly of the cavity to the waveguide, and was determined by measuring the required compressive force with a spring balance. Rf power was always removed from the sample during magnetic field movements which crossed the resonance field. Passage and equipment effects were eliminated by making downward as well as upward monitoring sweeps through resonance.

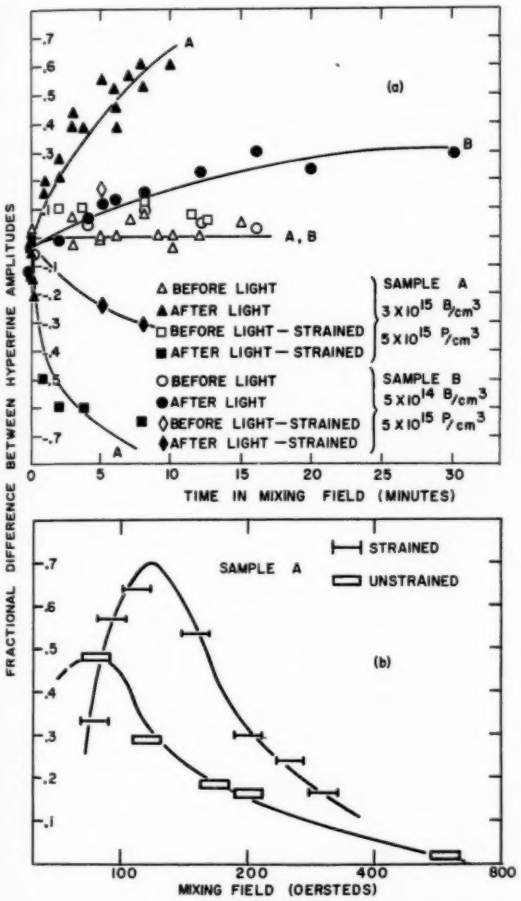

FIG. 2. (a) Relative difference of hyperfine amplitudes versus time in mixing field for two acceptor concentrations in phosphorus-doped silicon. (b) Experimental determination of optimum H_{mix} for strained and unstrained condition, sample A. Time in mixing field—strained, $3\frac{1}{2}$ minutes; unstrained, 6 minutes. (Data: $f_0\approx9000$ Mc/sec, $T=1.5°$K, Sample $A\approx5\times10^{15}$ P/cm^3, $\approx3\times10^{15}$ B/cm^3; Sample $B\approx5\times10^{15}$ P/cm^3, $\approx5\times10^{14}$ B/cm^3).

It has been pointed out[2,3] that the system of compensated donors and acceptors in a semiconductor offers excellent means of controlling the density of a paramagnetic species. This system also offers a means of adding or subtracting a species, for in this experiment it has been possible essentially to compare donor-electron relaxation times in the same sample with and without acceptors present.

I wish to express my appreciation for stimulating and enlightening conversations with E. O. Kane, C. Kittel, and R. Newman.

---

[1]G. Feher and E. A. Gere, Phys. Rev. 114, 1245 (1959), pp. 1254-55.

[2]A. Honig and R. Levitt, Phys. Rev. Letters 5, 93 (1960). The donor and acceptor concentrations in our sample were determined by a combination of Hall effect and spin resonance measurements as described in this Letter.

[3]G. Bemski (private communication).

[4]R. C. Fletcher, W. A. Yager, G. L. Pearson, A. N. Holden, W. T. Read, and F. R. Merritt, Phys. Rev. 94, 1392 (1954).

[5]A. Honig and E. Stupp, Phys. Rev. 117, 69 (1960).

[6]G. Feher, International Conference on Semiconductor Physics, Prague, 1960 (unpublished); G. Feher, J. C. Hensel, and E. A. Gere, Phys. Rev. Letters 5, 309 (1960). I am indebted to Dr. Feher for kindly furnishing me a preprint of his results on observation of spin resonance in acceptors in silicon in advance of publication.

[7]M. Weger, Bell System Tech. J. 39, 1013 (1960).

SENSITIVITY OF MICROWAVE SPECTROMETERS USING MASER TECHNIQUES

C. H. Townes*
Institute for Defense Analyses, Washington, D. C.
(Received October 10, 1960)

The minimum detectable absorption coefficient for an absorbing medium in a microwave waveguide has been written[1]

$$\alpha_{\min} = 2e\alpha_0(2k_e T_e \Delta\nu/P_0)^{1/2}, \quad (1)$$

where α_0 is the absorption coefficient per unit length of the waveguide, e the Napierian base, k Boltzmann's constant, P_0 the microwave power used, T_e the effective noise temperature of the amplifying system, and $\Delta\nu$ its bandwidth. Most microwave spectrometers have involved noise temperatures T_e of 10 000°K or greater. It is obvious that use of maser amplifiers can very much decrease T_e in expression (1) and thus improve spectrometer sensitivity. It will be shown here that additional large gains even beyond the reduction of T_e in expression (1) can be obtained by suitable use of maser-like techniques, assuming that sensitivity is limited only by random noise.

If the microwave power is sent into a perfect maser amplifier following partial absorption in a waveguide, one might expect that the noise temperature T_e would be as low as $h\nu/k$.[2] But this is not true, since the waveguide is normally at a temperature above $h\nu/k$ and radiates noise into the amplifier, making T_e comparable with the waveguide temperature T_g. Consider now the addition along the length of the waveguide of molecules in an excited state, which can undergo stimulated emission to a lower state. The noise radiated by the waveguide, including the excited molecules, is characterized by the temperature[2]

$$T_g' = \frac{h\nu}{k}\frac{a}{b-a}, \quad (2)$$

where a is the total probability of stimulated emission per unit time per photon and b is the total probability of absorption per unit time per photon. b includes all losses in the waveguide. As excited molecules are added, a approaches b and T_g becomes very large. However, the net absorption in the waveguide decreases since $\alpha_0 = (b-a)/C$, where C is the velocity of light, and hence $\alpha_{\min}$ appears to decrease without limit even with $\Delta\nu$ and P_0 fixed. A more complete analysis can be easily obtained with the help of expressions (14) and (15) of reference 2 for the waveguide case or of expressions (58) for the resonant cavity spectrometer.

If n_0 photons are introduced into a waveguide, the noise fluctuation when $b > a$ is

$$\Delta n = \left[n_0\left(\frac{a+b}{b-a}\right)\right]^{1/2} e^{(a-b)t/2}. \quad (3)$$

The signal due to a small change ϵ in $(b-a)$ associated with gas absorption is

$$S = n_0 e^{(a-b)t}\epsilon t. \quad (4)$$

If this is regarded as a peak signal, and the rms signal is equated to Δn, then $\Delta n = S/\sqrt{2}$. After optimization with respect to the time t, one has from (3) and (4)

$$\epsilon = e[2(b-a)(b+a)/n_0]^{1/2}. \quad (5)$$

A similar expression is obtained when $a > b$, except that $(b-a)$ becomes $(a-b)$. If b is due to normal absorption, then

$$b = \alpha_0(CkT_g/h\nu), \quad (6)$$

where T_g is the temperature of the waveguide walls. Furthermore $a \approx b$ so that (5) gives for the minimum detectable absorption coefficient

$$\alpha_{\min} = 2e(\alpha_0\alpha_0')^{1/2}(2kT_g\Delta\nu/P_0)^{1/2}. \quad (7)$$

Here $\alpha_0' = (b-a)/C$ can in principle be made as small as desired by adding excited molecules to increase a. The power level introduced into the waveguide is $P_0 = n_0 h\nu\Delta\nu$. Expression (7) should be compared with (1). When $T_e = T_g$, (1) gives approximately the best sensitivity obtainable by a perfect amplifier following the waveguide. (7) gives further increased sensitivity when excited atoms are added within the absorption cell. (7) also assumes that the following amplifier used is sufficiently good so that its effective noise temperature is much less than T_g', which is not impractical to achieve.

Consider now a cavity spectrometer, for which the minimum detectable absorption coefficient

is normally given by[3]

$$\alpha_{\min} \approx \frac{2\pi}{Q_c \lambda}\left(\frac{4kT_e \Delta\nu}{P_0}\right)^{1/2} \approx \frac{2}{\lambda}\left(\frac{2\pi kT_e \Delta\nu}{WQ_c\nu}\right)^{1/2}, \quad (8)$$

where Q_c is the cavity quality factor, λ the wavelength, and W the microwave energy stored in the cavity. Following Shimoda, Takahasi, and Townes,[2] the average number of photons in a cavity when $b > a$ is

$$\bar{n} = c/(b-a), \quad (9)$$

and the noise fluctuation is

$$\Delta n = (bc)^{1/2}/(b-a). \quad (10)$$

Here c is the probability per unit time of introduction of a photon by any process (including spontaneous emission) other than stimulated emission. The signal due to a small change ϵ in $b-a$ is from (9)

$$S = c\epsilon/(b-a)^2. \quad (11)$$

For signal equal to noise, from (10) and (11),

$$\epsilon_{\min} = (b/c)^{1/2}(b-a) = (bc)^{1/2}/\bar{n} = [(b-a)b/\bar{n}]^{1/2}. \quad (12)$$

The last form of (12) shows the similarity with expression (5) for the waveguide. Sensitivity is best when c is as small as possible, i.e., when $c = a$. Since also $a \approx b$, and $\bar{n} = W/h\nu$,

$$\epsilon_{\min} = b(n\Delta\nu/W)^{1/2}, \quad (13)$$

or

$$\alpha_{\min} = \frac{4\pi}{\lambda Q_c}\frac{kT_c}{h\nu}\left(\frac{h\Delta\nu}{W}\right)^{1/2}, \quad (14)$$

where T_c is the wall temperature of the cavity, and $b = 2kT_c/h\nu$.

Expression (14) is to be compared with (8). If a perfect amplifier is used outside the cavity, $T_e \approx T_c$ and (8) gives

$$\alpha_{\min} = \frac{2}{\lambda}\left(\frac{2\pi kT_c}{WQ_c}\frac{\Delta\nu}{\nu}\right)^{1/2}. \quad (15)$$

If the cavity is cooled so that $kT_c < h\nu$, then (8) may be written

$$\alpha_{\min} \approx \frac{2}{\lambda}\left(\frac{2\pi h\Delta\nu}{WQ}\right)^{1/2}. \quad (16)$$

The minimum detectable absorption coefficient given by (14), which applies when excited molecules are appropriately introduced directly into the cavity where absorption is to be detected, can hence be markedly less than the best achievable with external amplification alone, as given by either (15) or (16). It is interesting to express (14) in terms of the minimum detectable number of absorbing atoms or molecules. If a approaches b, spontaneous emission is amplified more and more and the bandwidth $\Delta\nu$ to which the cavity system will respond becomes smaller, since $\Delta\nu = \nu(b-a)/a$.[2] Let a approach b until W builds up to the point of saturation of the molecules to be detected. Then if α is expressed in terms of the total number of molecules N (in upper and lower states) producing the absorption, one can show that (14) gives for the minimum number N which can be detected in a time $1/\Delta\nu$

$$N_{\min} \approx \frac{16Q_L}{Q_c}\frac{kT_c}{h\nu}\frac{kT_N}{h\nu}, \quad (17)$$

where Q_c is the quality factor for the cavity before insertion of molecules in the excited state, and Q_L is $\nu/\delta\nu$ for the absorption line. Here the linewidth $\delta\nu$ is assumed due to relaxation processes alone; otherwise expression (17) is somewhat modified. T_N is the temperature of the absorbing material, which would usually be the same as T_c for the cavity walls, and we assume $kT_N \gg h\nu$. It is evident that some conditions allow detection of only a few molecules, if limitations are due to random noise only. Note also that (17) is independent of the matrix element for the absorption. The time required for detection of the number of atoms given by (17) is

$$t = 1/\Delta\nu = 3hV/(8\pi\mu^2 Q_L^2), \quad (18)$$

where μ^2 is the square of the matrix element for the transition being detected, and V the cavity volume. Thus the matrix element does affect the time required for such measurement. For $|\mu| = 10^{-18}$ esu, $V = 1$ cm^3, and $Q_L = 10^6$, (18) gives $t \approx 10^{-3}$ sec. Hence the time required for sensitivities indicated by (17) is not excessively long.

A spectrometer involving some of the above principles, utilizing excited molecules directly in the cavity and a change in $b-a$, has actually already been demonstrated without perhaps its potentiality and general applicability being fully realized. This was the experiment of Shimoda and Wang[4] on an oscillating beam-type maser. There the sensitivity was found to be much greater than that for an ordinary cavity-type spectrom-

eter; the factor of improvement obtained in practice was not precisely measured but was of the order of 50.

Various alternative situations can be worked out theoretically, and a number of types of arrangements to take advantage of the possibilities indicated above for increasing sensitivity can be rather easily seen. One such would be to insert paramagnetic material, for which a resonance is to be detected, into a microwave cavity at very low temperature and also containing ruby. The ruby would be "pumped" so that for it $a > b$, and for the entire cavity a approaches b until the system is approximately at the point of oscillation and the noise output is greater than that produced by any following amplifier. The desired resonance should be then detectable by sweeping it through the center of response of the cavity and excited ruby.

---

*On leave from Columbia University, New York, New York.

[1]C. H. Townes and A. L. Schawlow, Microwave Spectroscopy (McGraw-Hill Book Company, New York, 1955), p. 414.

[2]K. Shimoda, H. Takahasi, and C. H. Townes, J. Phys. Soc. Japan 12, 686 (1957).

[3]See reference 1, p. 437.

[4]K. Shimoda and T. C. Wang, Rev. Sci. Instr. 26, 1148 (1955).

FLUCTUATIONS OF NUCLEAR CROSS SECTIONS IN THE "CONTINUUM" REGION*

Torleif Ericson†
Lawrence Radiation Laboratory, University of California, Berkeley, California
(Received August 29, 1960; revised manuscript received October 14, 1960)

The assumption that the matrix elements of the compound nucleus are randomly distributed with respect to phase and magnitude has in recent years been very successful for the understanding of the fluctuations of the partial widths and the distribution of the level spacings of slow-neutron resonances.[1-3]

The purpose of this Letter is to examine the nontrivial consequences of the statistical assumption in the so-called "continuum" region, in which a large number of compound states overlap owing to the short lifetime of the compound nucleus. It is generally concluded that the excitation of a large number of intermediate compound states automatically implies that cross sections are smooth functions of the energy and that angular distributions are symmetrical around 90° to the beam direction. It will be shown that the proper statistical prediction for experiments performed with good energy resolution in the incident beam is that (1) partial cross sections and angular distributions fluctuate even though a large number of intermediate states are excited, (2) the formation and decay of the compound nucleus are independent only on the average, and (3) the fluctuations can be used to determine the lifetime of the compound nucleus in the "continuum" region.

Consider the compound-nucleus reaction proceeding from the initial state $|\alpha\rangle$—, i.e., the target nucleus and the incident wave—to the final state $|\alpha'\rangle$, a particular state of the final nucleus and the corresponding emitted wave. We assume the experiment to be performed with infinitely good energy resolution in the incident beam. The scattering matrix $S_{\alpha\alpha'}$ can be divided into two parts, one, S_α, leading into the compound nucleus, and one, $S_{\alpha'}$, leading out of the compound nucleus. The intermediate compound states $|i\rangle$ of energy E_i are excited with probability amplitudes $f(E, E_i)$ which are approximately of the form

$$f(E, E_i) \propto \frac{1}{(E - E_i) + i\Gamma/2}. \tag{1}$$

The "width" Γ depends in principle on the intermediate state $|i\rangle$. At high excitation this dependence will be weak, because Γ will be a sum of a large number of partial widths, of which no single one dominates. This situation should be realized at some 3-4 Mev above neutron binding energy in heavy nuclei, but is not very well realized at lower excitation. As we discuss the case of high excitation, we will neglect the fluctuations in Γ and take it to be a constant. The "width" Γ is related to the lifetime τ of the compound nucleus by $\Gamma = \hbar/\tau$ by the uncertainty principle. Equation (1) expresses that the compound states within a region of the order of Γ are excited simultaneously and must be treated coher-

ently; we therefore call Γ the coherence energy. The reaction cross section $\sigma_{\alpha\alpha'}(E)$ can be written

$$\sigma_{\alpha\alpha'}(E) \propto |\sum_i \langle \alpha | S_\alpha | i \rangle f(E, E_i) \langle i | S_{\alpha'} | \alpha' \rangle|^2. \quad (2)$$

The matrix elements $\langle \alpha | S_\alpha | i \rangle$ and $\langle i | S_{\alpha'} | \alpha' \rangle$, and consequently their product, have random phases. If the coherence energy Γ encompasses a large number of intermediate states $|i\rangle$, the sum in Eq. (2) consists of a large number of terms of random phases and becomes a random number, the real and imaginary part of which have Gaussian distributions. Therefore, if transitions to different final states are compared under otherwise identical conditions, the transition-matrix elements are independently random, because the factors $\langle i | S_{\alpha'} | \alpha' \rangle$ are uncorrelated and have uncorrelated phases. The partial cross sections $\sigma_{\alpha\alpha'}(E)$ therefore fluctuate essentially like neutron widths in spite of the large number of compound states excited.

Furthermore, intermediate states $|i\rangle$ are excited essentially only within the coherence energy Γ. If the incident energy is changed by an amount much larger than Γ, the intermediate states are entirely different. The matrix element, thus the cross section, is different from its previous value, in general. On the other hand, if the energy change is small compared with Γ, essentially the same states are excited; the matrix element and cross section are practically unchanged. As a measure of the region of energy over which the correlation in the cross section is important, we evaluate the mean value over E of $\sigma_{\alpha\alpha'}(E)\sigma_{\alpha\alpha'}(E+\epsilon)$ from Eq. (2):

$$\langle \sigma_{\alpha\alpha'}(E)\sigma_{\alpha\alpha'}(E+\epsilon) \rangle_{\text{av}} = \langle \sigma_{\alpha\alpha'}(E) \rangle_{\text{av}}^2 \left[1 + \frac{1}{1+(\epsilon/\Gamma)^2} \right]. \quad (3)$$

Therefore we conclude that a partial reaction cross section will fluctuate as a function of incident energy with a typical period of the order of the coherence energy Γ. Because Γ is directly related to the compound-nucleus lifetime, these fluctuations, in principle, provide a means for measuring the extremely short lifetime of highly excited nuclei.

We point out that the usual statement of independence of formation and decay of the compound nucleus is not valid in this type of experiment: The fluctuations do not necessarily occur at the same excitation energy, if the same compound nucleus is formed by different means. In the "continuum" region this independence is a consequence of averaging over many residual states, or over an energy interval much larger than the coherence energy.

A more exact discussion should include angular momentum. The main results remain unchanged. For the integrated partial cross sections, states of opposite parity contribute independently, slightly reducing the amplitude of the fluctuations. The partial angular distribution and polarization fluctuate as functions of the incident energy over energy regions of the order of Γ. Only after an average has been performed are the ordinary statements, of symmetry about 90° to the beam direction and no polarization, valid.

The total reaction cross section is usually a sum of a large number of fluctuating partial cross sections $\sigma_{\alpha\alpha'}$ and it will therefore usually have fluctuations of small amplitude only. When only few exit channels are available, the fluctuations are appreciable and occur also in the total cross section. Fluctuations in the total cross section have been observed by Cranberg[4] with high-resolution neutrons on Ti and Fe. At 2.5-Mev incident neutron energy and 2-kev resolution the total cross section exhibits a fine structure which, for Fe, has a half-width of 5 kev, corresponding to an approximate lifetime of 10^{-19} sec. The expected spacing of levels of spin 1/2 is indicated to be of the order of a few kev by slow-neutron resonances; the spacings of all excited states are considerably smaller.

---

*This work was done under the auspices of the U. S. Atomic Energy Commission.

†Present address: CERN, Geneva, Switzerland, on leave from the Institute of Theoretical Physics, Lund, Sweden.

[1]C. E. Porter and R. G. Thomas, Phys. Rev. 104, 483 (1956).

[2]E. P. Wigner, in Proceedings of the Conference on Neutron Physics by Time-of-Flight, Gatlinburg, Tennessee, 1956 [Oak Ridge National Laboratory Report ORNL-2309 (unpublished)].

[3]L. Landau and Y. Smorodinsky, lectures on the Theory of the Atomic Nucleus, Moscow, 1956 (unpublished).

[4]Dr. L. Cranberg (private communication). See also L. Cranberg et al., in Proceedings of the Conference on Neutron Physics by Time-of-Flight, Gatlinburg, Tennessee, 1956 [Oak Ridge National Laboratory Report ORNL-2309 (unpublished)], p. 148.

FREQUENCY DISTRIBUTION OF RESONANCE LINE VERSUS DELAY TIME

C. S. Wu, Y. K. Lee, N. Benczer-Koller, and P. Simms
Columbia University, New York, New York
(Received September 26, 1960)

In the quantum theory, the intensity distribution of a line emitted in a transition between two states with $\Delta E = \hbar\omega$ is given by

$$I(\omega)d\omega = \frac{\gamma}{2\pi}\frac{\hbar\omega d\omega}{(\omega-\omega_0)^2+\frac{1}{4}\gamma^2},$$

when the period of observation T is long compared to the mean lifetime T_{av} of the excited state. The distribution has a maximum intensity for the frequency ω_0 and the breadth at half maximum is equal to γ, the initial transition probability per unit time or the reciprocal lifetime, $\gamma = 1/T_{av}$. This distribution is identical with the natural line shape for emission and absorption of the light in a classical treatment where $\omega/2\pi$ is the frequency of an oscillator and the natural breadth γ is due to the damping force of the emitted radiation on the oscillator. Therefore, the quantum analog of the classical natural linebreadth γ is the initial transition probability per unit time. However, when the time T is short or comparable to the mean lifetime T_{av} of the excited state, the frequency spectrum of the emitted line follows the function

$$\frac{1+e^{-\gamma T}-2e^{-\gamma T/2}\cos(\omega-\omega_0)T}{(\omega-\omega_0)^2+\frac{1}{4}\gamma^2}.$$

The propagation of such a composite wave[1] through a dispersive medium filled with resonators like the resonance absorber depends on both the frequency distribution of the incident wave, which is governed by the duration of the wave train T, and the complex dielectric constant of the medium which can be affected by Doppler shift.

The unusual frequency-sensitivity of the Mössbauer effect[2] in Fe^{57} provides an excellent means to demonstrate such phenomena. In a recent paper Holland and his co-workers[3] reported their interesting results on the time spectra of filtered resonance radiation of Fe^{57}. The filtered resonance radiation displayed a nonexponential time decay as a consequence of the Fourier spectrum of the short wave train and the dispersive nature of the filtering medium.

Our approach to this investigation is to observe directly the resonance frequency spectrum of Fe^{57} at different time intervals T after the formation of the 14.4-kev excited state or classically the starting of the wave train. The detection of the preceding radiation (123-kev line) serves as the signal of the formation of the 14.4-kev excited state.

A theoretical treatment based on classical theory has been developed by Hamermesh[4] assuming a single emission and absorption line. (A quantum mechanical treatment[5] yields identical results.) For a Co^{57} source imbedded in a metallic iron environment, the 14.4-kev line of Fe^{57} has a hyperfine structure of six lines and so does the iron absorber. For very short delay times, each of the lines spreads to such an extent that the adjacent lines overlap each other. Under these circumstances, the simple assumption that each component interacts only with its own counterpart in the absorber is no longer valid. To overcome this complication a Co^{57} source electroplated onto a thin stainless steel foil (No. 302; 8.3 mg/cm^2) and a stainless steel absorber cut from the same foil were used. According to Wertheim's results[6] the spin correlation time in stainless steel is sufficiently short to exhibit an unsplit line. The single-peak resonance spectrum as shown in Fig. 1(c) confirms the absence of the satellites. The observed linewidth, after the correction for the absorber thickness, closely approaches the expected natural width, therefore dispelling the doubt that the spin correlation time may not be sufficiently short. Both source and absorber were annealed in hydrogen at approximately 1000°C for a period of several hours. The estimated fraction of nonrecoil emission or absorption (assuming $f = f'$) is nearly 60%.

A continuous range of Doppler shifts[7] are obtained by fixing the source to one end of a light metal tube which passes coaxially through two loud speakers that are rigidly bolted back to back. The paper cones of the speakers have been removed and the tube fastened to the two voice coils. The tube is otherwise unsupported so that it is free to follow the voice coil motion. The source is placed in motion by driving one of the voice coils with a sinusoidal oscillator (12-30 cps). The other coil follows the motion, and the induced sine wave is amplified and directly coupled into a multichannel analyzer which

serves as an instantaneous velocity indicator and recorder. Normalization is obtained by accumulating the velocity spectrum of the nonresonant line (123 kev) and the resonant line (14.4 kev) side by side on the multichannel analyzer. For the delayed coincidence investigation, the 14.4-kev resonance spectrum is gated by a fast-slow coincidence system operated by the 14.4-kev, and 123-kev line. The time-delay coincidence circuit is very similar to that of Green and Bell[8] with some minor improvements. The detectors used are thin NaI scintillation counters and the time resolution was determined from the prompt curve to be 25 mμsec. The source (5-mm diam) is placed 2 cm away from the absorber. The exposed area of the absorber is defined by a thick lead shield with an opening of 3-cm diameter. The 14.4-kev detector is 2 cm from the absorber and the 123-kev detector views the source sidewise at 3 cm.

Our results can be summarized in Figs. 1-3. In Fig. 1, three resonance spectra [1(a), 1(b), and 1(c)] are exhibited. They are Armco iron source (0.7 mil) with Armco iron absorber (0.3 mil), stainless steel source (No. 302; 8.3 mg/cm²) with Armco iron absorber (0.7 mil), and stainless steel source (No. 302; 8.3 mg/cm²) with stainless steel absorber (No. 302; 8.3 mg/cm²), respectively. The separations between the central line and the first pair of satellites in 1(a) and between the first and second satellite lines in 1(b) should be equal to each other and equal to the energy separation between the sublevels of the upper state. This measurement provides a convenient velocity calibration of our system because this separation is known from earlier direct "lathe" method. Curve 1(c) shows only a single, narrow line; therefore it fulfills our requirements. The most pronounced prediction of the theory is that the apparent width of the main resonance line is initially very broad and then compresses as the duration of the de-

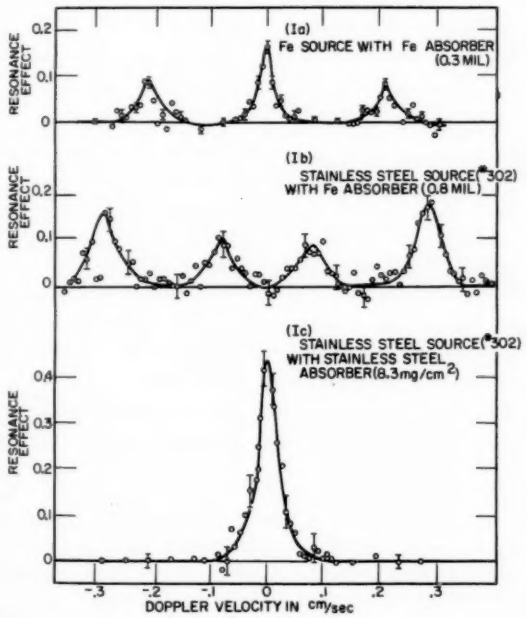

FIG. 1. Resonance effect of the 14.4-kev line from Fe^{57} imbedded in various source environments with various absorbers: (a) Co^{57} electroplated on Armco iron foil with Armco iron foil as absorber; (b) Co^{57} electroplated on stainless steel foil (No. 302) as source and Armco iron foil as absorber; (c) Same stainless steel foil (No. 302) used both as the backing material for the source and as absorber.

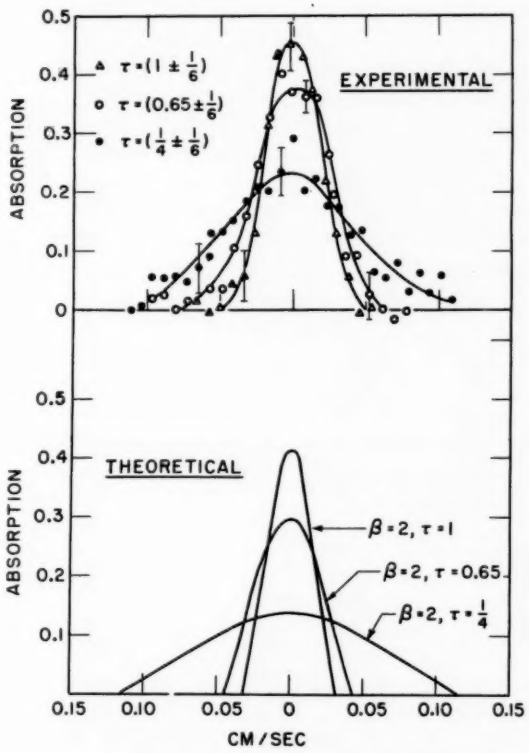

FIG. 2. The central resonance line versus delay time, where $\beta = N\sigma_0 f'$, and $\tau = T/T_{av}$. T is the delay time used. The upper portion shows the experimental results with delay times of $\tau = 1/4$, 0.65, and 1. The lower portion exhibits the theoretical curves calculated for the above delay times.

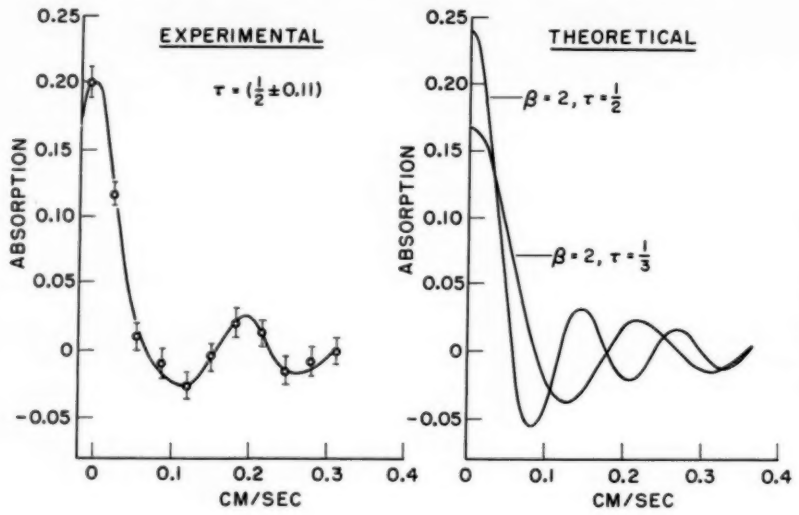

FIG. 3. The extended resonance spectrum for delayed coincidences at $\tau = T/T_{av} = (1/2 \pm 0.11)$ is shown on the left. The observed distribution falls somewhere between the two theoretical curves calculated for $\tau = 1/3$ as shown on the right.

layed time increases. To illustrate this point, the observed central resonance lines alone were plotted with various delayed time intervals, approximately 35 mμsec, 94 mμsec, and 150 mμsec as shown in Fig. 2. The theoretical curves for $\beta = 2$ and $T = \frac{1}{4}T_{av}$, $0.65T_{av}$, and T_{av} are plotted side by side for comparison.

The theoretical formula for the time dependence of the transmitted intensity derived by Hamermesh[4] involves the summation of Bessel functions:

$$|a'(\tau)|^2 = e^{-\tau}\left|\sum_{n=0}^{\infty}\left(i\frac{4}{\beta}\frac{\Delta\omega}{\gamma}\right)^n\left(\frac{\beta\tau}{4}\right)^{\frac{1}{2}n} J_n(\beta^{\frac{1}{2}}\tau^{\frac{1}{2}})\right|^2.$$

For large values of $\Delta\omega$ the transmitted intensity is

$$|a'(\tau)|^2 = e^{-\tau}\left|\exp\left[i\left(\frac{\Delta\omega}{\gamma}\tau + \frac{\gamma}{\Delta\omega}\frac{\beta}{4}\right)\right.\right.$$
$$\left.\left. + \sum_{n=1}^{\infty}\left(i\frac{\beta}{4}\frac{\gamma}{\Delta\omega}\right)^n\left(\frac{\beta\tau}{4}\right)^{-\frac{1}{2}n} J_n(\beta^{\frac{1}{2}}\tau^{\frac{1}{2}})\right|^2,$$

where $\beta = n\sigma_0 f'$ is the absorber thickness in terms of number of mean free paths (n = number of Fe^{57} atoms/cm^2, σ_0 = cross section at resonance, f' = the recoilless fraction of absorption) and $\tau = \gamma T = T/T_{av}$. However, for a thin absorber of $\beta = 2$ a series expansion of the exponential term in the amplitude function retaining the first three terms is quite sufficient for most purposes. This gives[9]

$$|a'(\tau)|^2 = \left[1 - \frac{\gamma\beta}{2}\frac{\sin(\Delta\omega T)}{\Delta\omega} + \left(\frac{\gamma\beta}{4}\right)^2\left\{\frac{1-\cos(\Delta\omega T)}{(\Delta\omega)^2} + \frac{T\sin(\Delta\omega T)}{\Delta\omega}\right\}\right]e^{-\tau}.$$

In our stainless steel case, the value of β calculated for the absorber is between 1 and 2. However, one must also take into account the source thickness but this is rather difficult to estimate without knowledge of the environment of the source. Furthermore, for precise comparison, the finite time resolution and the observed linewidth must be folded into the formula. This is rather involved and was not attempted. The effect of the delayed time interval on the linewidth as well as the amount of resonance effect is most apparent in Fig. 2 and it illustrates the points predicted theoretically.

As was previously stated, the absorber behaves like a resonant filter. It reverberates in response to the incident damped oscillation. For a wave train of short duration, the theoretical resonance spectrum for a single line predicts many repeated waves oscillating up and down across the zero-absorption axis with diminishing intensities as the Doppler frequency increases. Those portions of the spectrum extending below the zero-absorption axis imply the existence of a negative absorption, which means more radiation transmitted with absorber than without.

This interesting phenomenon was actually observed and the results for a delayed time interval of 80 mμsec are shown in Fig. 3(a) which is to be compared with the theoretical curves 3(b) calculated for $\beta = 2$ and $\tau = T/T_{av} = 1/2$ and $\tau = 1/3$. In order to observe this effect, the time resolution was improved to 15 mμsec in order to reduce the smearing effect due to the uncertainty in time resolution. The agreement is very good.

The authors are deeply indebted to Professor N. Kroll and Dr. M. Morita who theoretically formulated the behavior of the resonance effect versus delay time for us before we were aware of Hamermesh's calculation. We are particularly grateful to Professor W. Lamb, Jr., Professor H. Frauenfelder, and Dr. E. L. Garwin for their stimulating discussions. To many of our colleagues, H. Fleischman, H. Goldberg, and H. Dowds who have contributed in the preparation of the experiment, we express our thanks.

[1]In actual calculations for the dispersive phenomena the amplitude of the incident wave is used.

[2]R. L. Mössbauer, Z. Physik 151, 125 (1959); Naturwissenschaften 45, 538 (1958).

[3]R. E. Holland, F. J. Lynch, G. J. Perlow, and S. S. Hanna, Phys. Rev. Letters 4, 181 (1960). We are also indebted to the authors for the preprint of a more detailed paper: F. J. Lynch, R. E. Holland, and M. Hamermesh, Phys. Rev. 120, 513 (1960).

[4]M. Hamermesh, Argonne National Laboratory Summary Report ANL-6111, February, 1960 (unpublished).

[5]S. Harris, reported at the Symposium on Mössbauer Effect, Allerton House, University of Illinois, June 6 and 7, 1960 (unpublished).

[6]G. K. Wertheim, Phys. Rev. Letters 4, 403 (1960).

[7]This idea was originally suggested by S. DeBenedetti.

[8]R. E. Green and R. E. Bell, Nuclear Instr. 3, 127 (1958).

[9]W. Lamb, Jr. (private communication).

DOUBLE PION PHOTOPRODUCTION*

M. Feldman,† V. Highland, J. W. DeWire,‡ and R. M. Littauer
Laboratory of Nuclear Studies, Cornell University, Ithaca, New York
(Received October 7, 1960)

The photoproduction of two pions from hydrogen is interesting not only from the viewpoint of the isobar model[1] and pion-nucleon forces but for the study of pion-pion forces.[2] The possible reactions are

$$\gamma + p \rightarrow p + \pi^0 + \pi^0, \quad (1)$$

$$\gamma + p \rightarrow p + \pi^+ + \pi^-, \quad (2)$$

$$\gamma + p \rightarrow n + \pi^+ + \pi^0. \quad (3)$$

Various workers[3] have looked at the π^- from (2). Chasan et al.[4] observed all the particles from (2) in a cloud chamber. Recently Silverman and Richert[5] observed the recoil proton and one of the π's from (1) and (2).

We have used the bremsstrahlung beam of the Cornell synchrotron to observe (1) and (3) by detecting the two π's in coincidence. A photon from the decay of a π^0 enters the totally absorbing lead glass Čerenkov counter C (Fig. 1), producing a pulse proportional to its energy. An anticoincidence counter, A, prevents charged particles from being counted. Because the π^0 decays into a spectrum of photons, there is no sharp energy threshold for its detection. With a 150-Mev bias on the photon energy, the efficiency for detecting

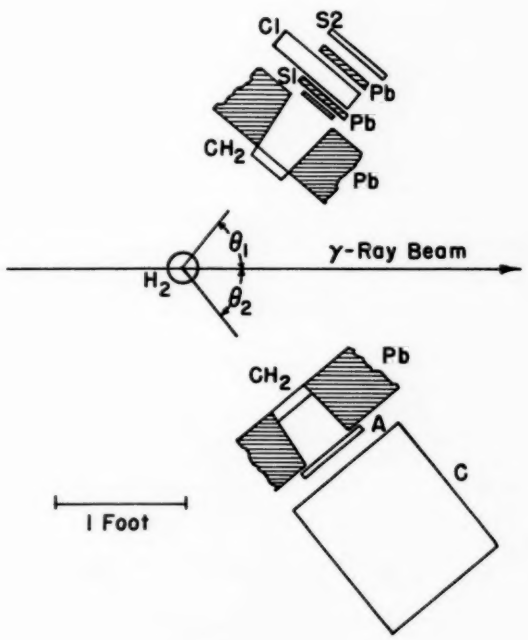

FIG. 1. Experimental arrangement.

a π^0 rises from 0 at a total energy of 185 Mev to 1.0 at 300 Mev and 1.5 at 600 Mev. The angular spread of the π^0 decay is about $\pm 15°$. A correction of about 10% arising from this spread has not been made, but does not vary rapidly with the π^0 angle.

For reaction (1) two total absorption Čerenkov counters are used. Because of the wide angle and high-energy bias a pair of photons from the decay of a single π^0 cannot be counted.

The π^+ in reaction (3) enters a telescope consisting of two scintillation counters and a Lucite Čerenkov counter ($S1$, $S2$, and $C1$). The Čerenkov counter detects π's of energy $\gtrsim 90$ Mev, but prevents protons produced in coincidence with single π^0's from being counted. Corrections of about 20% have been made for nuclear absorption of the π's in the absorbers and counters.

With a 2×10^{-8}-sec resolving time the correction for random electrons or pions in the telescope was ~15%.

Corrections of 5 to 10% were made for photon conversion in the polyethylene absorbers. Triple meson production is small[4] and has been neglected.

Because a given pion lab angle transforms into a spectrum of angles in the center-of-mass system all our data will be presented in the lab system. The data are also shown divided by the Lorentz-invariant three-body phase space factor[6] given by

$$D(\theta_1,\theta_2) = C\int \frac{dP_1}{E_1E_2E_p}\,\frac{E_2E_pP_2{}^3P_1{}^2F_1F_2}{P_2{}^2(E_2+E_p)-E_2P_2\cdot(P_2+P_p)}. \quad (4)$$

The integral is taken over the momentum of the first π. F_1 and F_2 are the detection efficiencies for the first and second π's.

The results are given in Fig. 2 and Table I. The gamma-ray interval from 930 to 1200 Mev was obtained by subtracting bremsstrahlung spectra. Reaction (1) seems to be isotropic. Reaction (3) shows a strong forward peaking of the π^+, particularly for forward π^0 angles. Drell[7] has suggested a process with a forward π^+ dis-

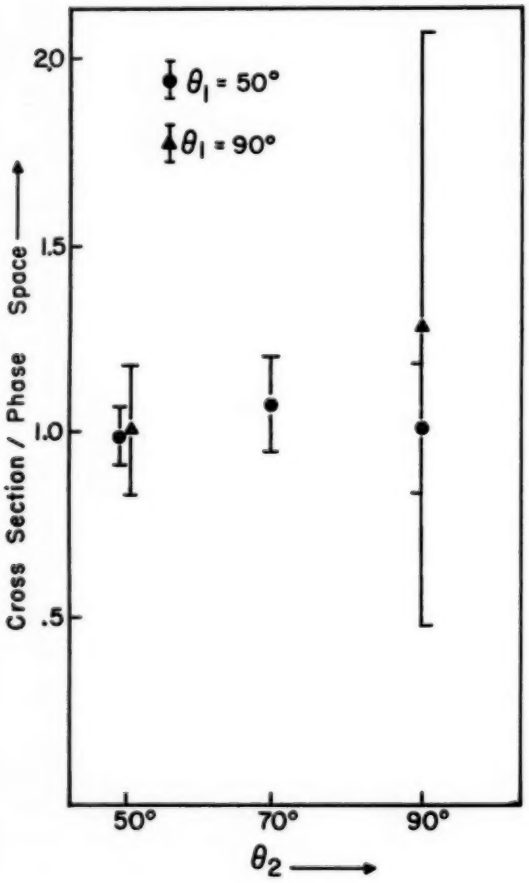

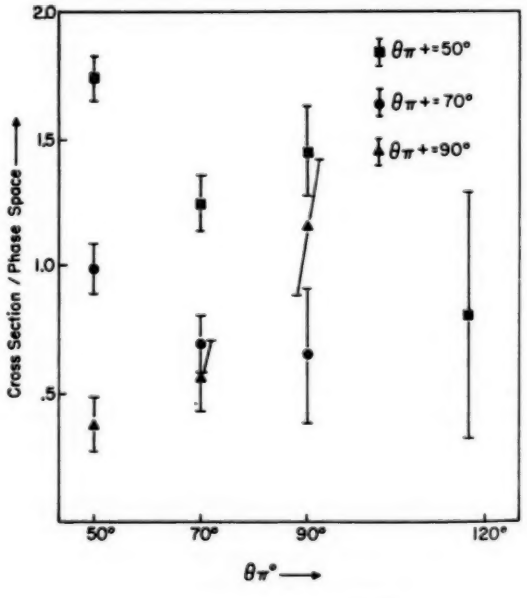

FIG. 2. (a) $\pi^0+\pi^0$ results divided by phase space factor; (b) $\pi^+ + \pi^0$ results divided by phase space factor.

Table I. Experimental results and comparison with phase space for the gamma-ray interval 930-1200 Mev. $T_{\pi^+} \gtrsim 90$ Mev; $T_{\pi^0} \gtrsim 125$ Mev.

π^0 angle	π^+ angle			π^0 angle	
	50°	70°	90°	50°	90°
	Lab cross section in 10^{-30} cm^2/sr^2				
50°	1.36 ± 0.07	0.46 ± 0.05	0.09 ± 0.02	1.05 ± 0.09	0.28 ± 0.05
70°	0.53 ± 0.05	0.14 ± 0.02	0.05 ± 0.01	0.62 ± 0.07	
90°	0.30 ± 0.04	0.05 ± 0.02	0.04 ± 0.01	0.28 ± 0.05	0.05 ± 0.03
120°	0.05 ± 0.03			0.07 ± 0.10	
	Cross section divided by phase space factor, arbitrary units				
50°	1.74 ± 0.09	0.99 ± 0.10	0.38 ± 0.11	0.99 ± 0.08	1.01 ± 0.17
70°	1.24 ± 0.11	0.69 ± 0.12	0.57 ± 0.14	1.07 ± 0.12	
90°	1.5 ± 0.2	0.7 ± 0.3	1.2 ± 0.3	1.01 ± 0.17	1.3 ± 0.8
120°	0.8 ± 0.5			1 ± 1	

tribution; however, the mean lab angle would be only 8°.

When the π^+ angle is 90°, the π^0 distribution is peaked backwards.

Below 930 Mev, $\pi^0+\pi^0$ production is depressed at the 50°-50° point, while $\pi^+ + \pi^0$ production is depressed at the 90°-90° point.

The special case when the π's are produced at symmetrical angles is interesting because the energy between the π's in their own center-of-mass system is nearly independent of the energy of either of the π's. To a lesser extent this is also true of the pion-nucleon energies. The 50°-50° and 70°-70° points (Table II) have nearly the same pion-pion energy (the spread arises mainly from the spread in incident photon energies). However, the pion-nucleon energy for the 50°-50° point includes the 3/2-3/2 resonance while that of the 70°-70° point does not; this probably explains why the 50°-50° point is higher. Work is continuing at other energies in the hope of separating the pion-pion effects.

Table II. The symmetrical cases of $\pi^+ + \pi^0$ production. Note that the energies are in the center-of-mass systems.

Pion angles	50° - 50°	70° - 70°	90° - 90°
$\left(\frac{\text{Cross section}}{\text{phase space factor}}\right)$	1.74 ±0.09	0.69 ±0.12	1.2 ±0.3
$E_{\pi+\pi}$ (Mev)	660 - 810	640 - 760	540 - 610
$E_{\pi+N} - m_p$ (Mev)	190 - 480	420 - 660	610 - 840

*Supported by the joint program of the Office of Naval Research and the U. S. Atomic Energy Commission.

†National Science Foundation predoctoral fellow.

‡On leave of absence at the Istituto Nazionale di Fisica Nucleare, Frascati, Italy.

[1]R. F. Peierls, Phys. Rev. 118, 325 (1960); 111, 1373 (1958).

[2]S. D. Drell and F. Zachariasen, Phys. Rev. Letters 5, 66 (1960).

[3]For example, M. Bloch and M. Sands, Phys. Rev. 108, 1101 (1957); W. Woodward, R. R. Wilson, and D. Luckey, Proceedings of the Seventh Annual Rochester Conference on High-Energy Nuclear Physics, 1957 (Interscience Publishers, New York, 1957), p. 42.

[4]B. M. Chasan, G. Cocconi, V. T. Cocconi, R. M. Schechtman, and D. H. White, Phys. Rev. 119, 811 (1960).

[5]S. Richert and A. Silverman, Bull. Am. Phys. Soc. 5, 237 (1960).

[6]P. Carruthers (private communication).

[7]S. D. Drell, Phys. Rev. Letters 5, 278 (1960), and private communication. A $\pi^+\pi^-$ pair is photoproduced in vacuum and the π^- charge exchanges with a proton.

EXTRAPOLATION METHOD TO DETERMINE DIFFERENTIAL SCATTERING CROSS SECTIONS OF UNSTABLE PARTICLES*

Michael Nauenberg†
Lawrence Radiation Laboratory, University of California, Berkeley, California
(Received October 3, 1960)

Chew and Low[1] and Goebel[2] have discussed a method to measure the cross sections for scattering of particles such as pions and neutrons which are not available as free targets in the laboratory. The method consists of extrapolating the cross section for a related but measurable reaction as a function of one of the invariant momentum transfers to a pole of the S matrix for this reaction. The success of the extrapolation depends on the location and strength of other less well known singularities of the S matrix. In this note we want to point out the existence of two branch points which appear in the Chew-Low prescription for extrapolation to obtain the differential cross section of the unstable particle. These branch points are due to the constraint of fixed scattering angle, and disappear only when the integration over angle to obtain total cross sections is carried out. We will indicate how to modify the extrapolation to avoid this difficulty.

Suppose we want to measure the differential scattering cross section for the process

$$a_1 + a_2 \to a_3 + a_4, \tag{1}$$

where a_2 is emitted virtually by the process

$$a_6 \rightleftharpoons a_2 + a_5. \tag{2}$$

Then, according to Chew and Low, we measure the cross section for the reaction

$$a_1 + a_6 \to a_5 + a_3 + a_4,$$

and extrapolate it in the momentum transfer $S_{56} = (q_6 - q_5)^2$ to the value $S_{56} = m_2^2$, keeping fixed $S_{34} = (q_3 + q_4)^2$, the square of the total energy of a_3 and a_4, and $\cos\theta_{14}$, the cosine of the angle between a_1 and a_4, both in the rest frame of a_3 and a_4. The variables q_i and m_i refer to the four-momentum and mass of the particle a_i. In the limit $S_{56} \to m_2^2$, the laboratory-system cross section for this reaction takes the form[1]

$$d\sigma = \frac{\Gamma^2}{4\pi}\frac{m_5}{m_6 q_1^2}\frac{\{[S_{34} - (m_1 - m_2)^2][S_{34} - (m_1 + m_2)^2]\}^{1/2}}{(S_{56} - m_2^2)^2} \times \frac{d\sigma_0}{d\Omega_4}(S_{34}, S_{14})\, d\Omega_4\, dS_{34}\, dS_{56}, \tag{3}$$

where $d\sigma_0/d\Omega_4$ is the differential cross section for Process (1) and $(4\pi)^{1/2}\Gamma$ is the amplitude for Process (2) (coupling constant). For fixed S_{34} and $\cos\theta_{14}$, the invariant momentum transfer $S_{14} = (q_1 - q_4)^2$ is a function of S_{56},

$$S_{14} = m_1^2 + m_4^2 - \frac{1}{2S_{34}}\{(S_{34} + m_1^2 - S_{56})(S_{34} + m_4^2 - m_3^2) - [[S_{34} - (m_3 - m_4)^2][S_{34} - (m_3 + m_4)^2] \times [S_{56} - ((S_{34})^{1/2} - m_1)^2][S_{56} - ((S_{34})^{1/2} + m_1)^2]]^{1/2}\cos\theta_{14}\}.$$

Evidently S_{14} is analytic in S_{56} except for square-root branch points at $S_{56} = [(S_{34})^{1/2} \pm m_1]^2$. Since $d\sigma_0/d\Omega_4$ is analytic in S_{14}, it has also branch points at the same location when considered as a function of S_{56}. However, integration over the scattering angle θ_{14} to obtain the total cross section removes these branch points. This can be seen, for instance, by expanding $d\sigma_0/d\Omega_4$ in a Taylor series in S_{14}, noticing that only even powers of $\cos\theta_{14}$ contribute to the integration.

We note that the minimum experimental value of $(S_{34})^{1/2}$ is $(m_3 + m_4)$. On the other hand, in order that the branch points do not lie between the measured values of S_{56} ($S_{56} < 0$) and its value at the pole ($S_{56} = m_2^2$), it is necessary to consider $(m_1 + m_2) < (S_{34})^{1/2}$. For the case $m_3 + m_4 < m_1 + m_2$, these branch points would forbid extrapolation to the unphysical but interesting region $(m_3 + m_4) < (S_{34})^{1/2} < (m_1 + m_2)$ (for example, in the measurement of $K + K \to \pi + \pi$ by extrapolating $K + N \to Y + \pi + \pi$).

These branch-point singularities can be avoided by using the invariant momentum transfer S_{14} instead of S_{56} as the variable of extrapolation. Inverting Eq. (4), we express S_{56} as a function of S_{14} for fixed S_{34} and $\cos\theta_{14}$, and substitute it in Eq. (3). Square-root branch points in S_{14} appear now explicitly in Eq. (3), and can be treated exactly. Another alternative is to keep S_{14} instead of $\cos\theta_{14}$ fixed. Since the ranges of values of S_{14} in the physical region of Reactions (1) and (3) are not the same, it will be necessary to perform a second extrapolation, this time for $d\sigma_0/d\Omega_4$ as a function of S_{14} (i.e., $\cos\theta_{14}$), in order to obtain the differential scattering cross section in the nonoverlapping region. On the other hand, this method allows us by extrapolation in S_{56} to obtain the differential cross section $d\sigma_0/d\Omega_4$ in an unphysical range of S_{14}.

I would like to thank Professor Geoffrey F. Chew and Dr. B. M. Udgaonkar for several helpful discussions.

*This work was performed under the auspices of the U. S. Atomic Energy Commission.

†Present address: Institute for Advanced Study, Princeton, New Jersey.

[1]G. Chew and F. Low, Phys. Rev. 113, 1640 (1959).

[2]C. Goebel, Phys. Rev. Letters 1, 337 (1958).

P-WAVE PHASE SHIFTS AT 210 MEV AND THE PHOTODISINTEGRATION OF THE DEUTERON*

Gustav Kramer†

School of Physics, University of Minnesota, Minneapolis, Minnesota

(Received August 31, 1960)

It has recently been shown that the cross section for photodisintegration of the deuteron can give useful information about the nuclear force in the ^3P state if the following assumptions are made: (1) The ground-state wave function is known. (2) The electric dipole process $^3S_1+^3D_1-^3P_0$, $^3P_1$, $^3P_2+^3F_2$ is dominant. (3) Virtual meson effects can be neglected.[1,2]

The angular distribution of protons or neutrons produced in the photodisintegration of the deutron has the general form (in the c.m. system):

$$d\sigma/d\Omega = a + b\sin^2\theta + c\cos\theta + d\sin^2\theta\cos\theta + f\sin^4\theta.$$

For γ-ray energies corresponding to n-p scattering of 150 Mev it has been found in references 1 and 2 that the calculated values of a/b are only in satisfactory agreement with the experimental data provided the ^3P phase shifts are as characterized by a repulsive long-range tensor potential [$\delta(^3P_0) > 0$, $\delta(^3P_1) < 0$, and $\delta(^3P_2) > 0$].

Besides the 310-Mev data the most extensive information about the nucleon-nucleon scattering phase shifts has been obtained at 210 Mev.[3] Mac Gregor and Moravcsik applied the modified phase-shift analysis program[4,5] to the Rochester proton-proton scattering data.[6-10] They found four sets of phase shifts (A, B, C, and D) from which they have excluded A and D on the ground that neither corresponds to one of the acceptable phase-shift solutions at 310 Mev.[4,5] Now, recent data on the depolarization parameter $D(\theta)$ show very clearly that solutions A and D are excluded by measurements at 210 Mev alone.[11] These data also indicate some preference for solution B over C.

From the point of view that nuclear forces are charge independent it is interesting to see whether deuteron photodisintegration data distinguish between the two sets B and C. Nucleon-nucleon scattering at 210 Mev corresponds to a γ-ray energy of 107.3 Mev. For this energy we claim that the three assumptions are still justified. The wave function of the ground state is fairly well known from studies of low-energy phenomena.[12] We choose the phenomenological deuteron wave functions of Hulthén and Sugawara,[12] which are fitted to given values of binding energy, quadrupole moment, deuteron effective range, and D-state probability, assuming a definite value for the hard-core radius in the n-p potential. For the binding energy and the quadrupole moment experimental values are taken. For the deuteron effective range we assume the experimental value of the triplet effective range which corresponds to the shape-independent approximation. The D-state probability p_D is not exactly known. From the magnetic moment of the deuteron one gets as an estimate for p_D the value 0.04, which we choose for our calculation. For the hard-core radius we take 0.43 f. The electric quadrupole transitions are only important for the asymmetry parameters c and d. Their contributions to a and b are 0.06 μb and 0.58 μb, respectively, if calculated in Born approximation. This is in agreement with results of Zernik, Rustgi, and Breit for $E_\gamma = 102.2$ Mev.[13] The contribution to f is nearly equal to the negative value of b. Because in the experimental analysis of the angular distribution the term proportional to $\sin^4\theta$ has not been taken into account, we can neglect this contribution to b. Only a very small contribution from the magnetic quadrupole transitions $^3S_1+^3D_1-^3P_1$, $^3P_2+^3F_2$ are expected as can be seen for $E_\gamma = 77.3$ Mev from the results of Kramer and Werntz.[14] But we take into account the interference of the magnetic quadrupole transitions with the electric dipole transitions which gives a significant increase of a and an equivalent decrease of b because of the relation $b = -\frac{3}{2}a$ for this interference.[14] The minor role of the magnetic dipole transitions has been established by

Table I. Phase-shift fits to 210-Mev data in degrees.

Sol.	$^1S_0$	$^1D_2$	$^3P_0$	$^3P_1$	$^3P_2$	$^3F_2$	C_2
A	12.8	0.5	-32.0	23.0	11.0	-12.1	7.7
B	5.9	7.5	2.1	-20.9	21.9	-10.3	-5.3
C	-15.7	2.8	-28.4	-2.1	30.2	-11.1	-17.8
D	-2.0	5.3	-41.6	-13.0	18.6	-8.4	-20.7

several authors.[2,13-15] From these calculations we can expect that the singlet transition contributes only a negligible amount to a and contributes a value near 0.7 μb to b. Because the singlet phase shifts of the four sets differ very little, we must expect these contributions for all four sets A, B, C, and D. We believe that virtual meson effects are not yet important at 107-Mev γ-ray energy which is still far below the meson production threshold. Furthermore, we refer to the investigation of Pearlstein and Klein.[16] These authors find, using conventional meson-theoretic methods, that virtual meson effects play only a very small role at γ-ray energies near 100 Mev.

In Table I we quote the phase shifts of the sets A, B, C, and D found by MacGregor and Moravcsik,[3] but converted to phase shifts as defined by Blatt and Biedenharn. Although the solutions A and D are excluded from proton-proton scattering data alone, we have done the calculations for them also. For the computation we have used the formulas of reference 2. Actually we do not know the potentials from which the radial wave functions of the final state can be calculated producing the four phase-shift sets. But, as was discussed earlier,[2] the electric dipole radial integrals do not depend strongly on the shape of the final-state wave function for small r, whereas beyond the range R of the nuclear potential the radial function has its asymptotic form which is completely defined by the phase shifts. Inside the range R we approximate the wave function by $\cos\delta_{lj}\, j_l(kr)$, where δ_{lj} is the phase shift and $j_l(kr)$ is the spherical Bessel function. For γ-ray energies up to 77 Mev we found that this approximation gives nearly the same result as the often used method of taking the asymptotic form for $r < R$.[2] For these γ-ray energies and for one specific phase-shift set it was shown that the approximation used here gives similar results to the exact treatment with actual potentials.[2,14,17] For R we choose the value 1.40 f. Retardation effects are taken into account partially. The small contribution of the function $S_2(qr)$ as defined in reference 14 is neglected, which is justified from the results of this reference.

The results for the four sets A, B, C, and D are 0.26 μb, 3.07 μb, 1.12 μb, and 1.30 μb for a and 2.02 μb, 0.36 μb, 2.45 μb, and 1.64 μb for b. If combined with the expected contribution for the $M1$ transition, we get for a/b the values 0.096, 2.9, 0.36, and 0.56, respectively. The experimental data[18-22] between 60-Mev and 150-Mev γ-ray energy are collected in Fig. 1. Figure 1 shows that only solution B yields a large enough value for a/b to be in agreement with the experiments. All other solutions give values for a/b which are smaller than the measured ones. This confirms that at 210 Mev a large negative $^3P_1$ phase shift can account for a large isotropic term in the deuteron photodisintegration, as has also been found at 150 Mev in references 1 and

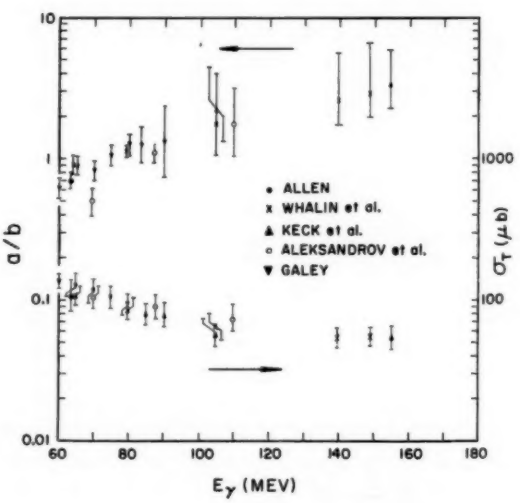

FIG. 1. Experimental data for a/b and σ_t.

2. Our calculations, however, are based on a hard-core radius 0.43 f and a D-state probability of 4%. It is clear that the ratio a/b does not depend strongly on the hard-core radius. But, of course, it is possible to get larger values for a if one increases the D-state admixture p_D. In Born approximation a is proportional to $\sqrt{p_D}$. If this dependence is verified in general, we must increase p_D at least by a factor of 4 to obtain $a/b=1$ for the phase shift sets A, C, and D. Such a large D-state admixture seems to be unreasonable. So, we arrive at the same conclusion concerning the sets A and D as Gotov and Heer[11] from their analysis of proton-proton scattering. But furthermore we have evidence that solution C must also be excluded.

The values predicted for the total cross section σ_t for the four sets A, B, C, and D are 26 μb, 48 μb, 41 μb, and 36 μb, respectively, whereas the measured value at $E_\gamma = 105$ Mev is (60 ± 10) μb,[19-21] as can be seen from Fig. 1. This shows that the dipole process yields the largest contribution for all sets of phase shifts. The smaller contribution to σ_t for the sets A, C, and D compared to the value for set B indicates a further preference for set B.

The author wishes to thank Edward Jezak for his interest and his assistance with the numerical calculations. The aid of the staff of the Computing Center of the University of Minnesota is gratefully acknowledged.

---

*Supported by the U. S. Atomic Energy Commission.

†On leave of absence from Institut für Theoretische Physik der Universität, Heidelberg, Germany.

[1]J. J. de Swart and R. E. Marshak, Physica 25, 1001 (1959).

[2]G. Kramer, Nuclear Phys. 15, 60 (1960).

[3]M. H. MacGregor and M. T. Moravcsik, Phys. Rev. Letters 4, 524 (1960).

[4]P. Cziffra, M. H. MacGregor, M. T. Moravcsik, and H. P. Stapp, Phys. Rev. 114, 880 (1959).

[5]M. H. MacGregor, M. T. Moravcsik, and H. P. Stapp, Phys. Rev. 116, 1248 (1959).

[6]E. Baskir, E. M. Hafner, A. Roberts, and T. H. Tinlot, Phys. Rev. 106, 564 (1957).

[7]T. Tinlot, E. Heer, A. England, and W. Gibson, Bull. Am. Phys. Soc. 4, 242 (1959).

[8]A. England, W. Gibson, E. Heer, and T. Tinlot, Bull. Am. Phys. Soc. 5, 76 (1960).

[9]C. L. Oxley and R. D. Schamberger, Phys. Rev. 85, 416 (1952).

[10]O. A. Towler, Phys. Rev. 85, 1024 (1952).

[11]K. Gotov and E. Heer, Phys. Rev. Letters 5, 111 (1960).

[12]L. Hulthén and M. Sugawara, Handbuch der Physik, edited by S. Flügge (Springer-Verlag, Berlin, 1957), Vol. 39.

[13]W. Zernik, M. L. Rustgi, and G. Breit, Phys. Rev. 114, 1358 (1959); M. L. Rustgi, W. Zernik, G. Breit, and D. T. Andrews (to be published).

[14]G. Kramer and C. Werntz, Phys. Rev. 119, 1627 (1960).

[15]B. Banerjee, G. Kramer, and L. Krüger, Z. Physik 153, 630 (1959).

[16]L. D. Pearlstein and A. Klein, Phys. Rev. 118, 193 (1960).

[17]T. T. de Swart and R. E. Marshak, Phys. Rev. 111, 272 (1958).

[18]L. Allen, Jr., Phys. Rev. 98, 705 (1955).

[19]J. C. Keck and A. V. Tollestrup, Phys. Rev. 101, 360 (1956).

[20]E. A. Whalin, B. D. Schriever, and A. O. Hanson, Phys. Rev. 101, 377 (1956).

[21]U. A. Aleksandrov, N. B. Delone, L. I. Slovokhotov, G. A. Sokol, and L. N. Shtarkov, J. Exptl. Theoret. Phys. U.S.S.R. 33, 614 (1958) [translation: Soviet Physics-JETP 6(33), 472 (1958)].

[22]J. A. Galey, Phys. Rev. 117, 763 (1960).

[23]J. Gammel and R. Thaler, Phys. Rev. 107, 291, 1337 (1957).

DETERMINATION OF THE RELATIVE Σ - Λ PARITY AND OF THE RATIO OF ASYMMETRY COEFFICIENTS α_Λ TO α_0 IN HYPERON DECAY FROM THE PION-HYPERON RESONANCE

Ph. Meyer,* J. Prentki, and Y. Yamaguchi†
CERN, Geneva, Switzerland
(Received October 10, 1960)

Recent evidence[1] for the existence of a pion-hyperon resonance Y^* of isospin 1 and mass ~1370 Mev leads to the possibility of determining the relative Σ - Λ parity and the ratio of asymmetry coefficients α_Λ (in $\Lambda \to p + \pi^-$) to α_0 (in $\Sigma^+ \to p + \pi^0$). In this Letter some experiments are proposed which allow the determination of the above-mentioned quantities by measuring only up/down asymmetries.

In what follows we shall suppose that the following conditions are satisfied:

(I) The isobar Y^* is a "good" resonance, meaning that it is reasonably narrow and pronounced so that experimental conditions can be chosen under which the resonant process dominates.

(II) In the "decay" of Y^*, for instance,

$$Y^{*+} \; (I=1) \to \begin{cases} \Lambda + \pi^+ & (a) \\ \quad \searrow\, p + \pi^- & (a') \\ \Sigma^0 + \pi^+ & (b) \\ \quad \searrow\, \Lambda + \gamma & (b') \\ \qquad \searrow\, p + \pi^- & (b'') \\ \Sigma^+ + \pi^0 & (c) \\ \quad \searrow\, p + \pi^0 & (c') \end{cases}$$

the branching ratio[2] $(b)/(a) = (c)/(a)$ is not too small.

Preliminary experiments seem to indicate that assumptions (I) and (II) are reasonable.

In pion phenomena the 33 resonance has played an eminent role in helping to understand pion physics. Should our assumptions be confirmed experimentally, then the Y^* resonance(s) may play a corresponding role in strange particle physics.

Consider, for instance, the reaction caused by monoenergetic pions:

$$\pi^+ + p \to K^+ + Y^{*+}, \tag{1}$$

with subsequent and immediate decay of Y^* according to (a), (b), and (c). Therefore what is actually observed is, for instance, the reaction

$$\pi^+ + p \to K^+ + \pi + \Lambda(\Sigma). \tag{2}$$

[It is clear that for our purpose one could also use

$$K^- + p \to \pi^- + Y^{*+}, \text{ etc...}$$

instead of (1).] Knowing the position of the resonance Y^*, it is possible to select[3] among (2) the K^+ associated with the resonant channel (1). The analysis which follows will always refer to such processes. In this way the plane formed by the incident π^+ and the outgoing K^+ is fixed once and for all. This plane S we shall refer to as the production plane.

Now let us define the quantities P_Λ and P_Σ as the "average" polarization of Λ's and Σ's coming via resonant reaction (1). This means that an average is made over all directions of hyperons, keeping the energy and direction of the associated K^+ fixed. As a consequence $\vec{P}_\Lambda$ and $\vec{P}_\Sigma$ are normal to the plane S.

Calling $\Pi(\Lambda)$, $\Pi(\Sigma)$, and $\Pi(Y^*)$ the parity of Λ, Σ, and Y^*, respectively (only relative parities are relevant), the following statements can be proved[4]:

(i) If $\Pi(\Lambda) = \Pi(\Sigma)$, then

$$P_\Lambda / P_\Sigma = +1, \tag{3}$$

for arbitrary spin J of Y^*.

(ii) If $\Pi(\Lambda) = -\Pi(\Sigma)$, then

$$P_\Lambda / P_\Sigma = \begin{cases} -1/3 \; (-5/3) \\ -3 \; (-3/5) \end{cases}$$

$$\text{for } J = 1/2 \; (3/2) \text{ and } \begin{cases} \Pi(\Lambda) = \Pi(Y^*) \\ \Pi(\Lambda) = -\Pi(Y^*). \end{cases} \tag{4}$$

In general $P_\Lambda / P_\Sigma < 0$ for any J and $\Pi(Y^*)$.[5]

As a result of (3) and (4) it is then sufficient to measure the sign of P_Λ / P_Σ in order to get the relative Σ - Λ parity.

However, what can be most easily measured is the up/down asymmetries with respect to the production plane S of the pions coming from the hyperon decays (a'), (b''), and (c'). Such measurements will provide us with, e.g., the ratio

$$\alpha_\Lambda P_\Lambda / \alpha_0 P_{\Sigma^+} \equiv n, \text{ etc.} \tag{5}$$

If we suppose that $\alpha_\Lambda / \alpha_0$ is known from other experiments, then by measuring n one obtains P_Λ / P_Σ and hence the Σ - Λ parity.

However, and this is to be stressed, it is possible to obtain separately P_Λ / P_Σ and $\alpha_\Lambda / \alpha_0$ by

considering the whole set of reactions (*a*), (*b*), and (*c*). This is essentially due to the fact that the same intermediate Y^* (because of the chosen experimental conditions) decays into the 3 channels.

(A) First of all, it is well known that in the decay $\Sigma^0 \to \Lambda + \gamma$ one has the relation $P_\Lambda = -\frac{1}{3} P_{\Sigma^0}$ if an average is made over all directions of Λ's, independently of the Σ - Λ relative parity.[6] Now let us consider the Λ's coming from reactions (*a*) and (*b'*). By measuring the up/down asymmetry in the decay of the Λ's in both cases, one can get the ratio

$$\frac{\alpha_\Lambda P_\Lambda}{\alpha_\Lambda P_{\Lambda\text{ind}}} = \frac{\alpha_\Lambda P_\Lambda}{\alpha_\Lambda (-\frac{1}{3} P_{\Sigma^0})} = -3 \frac{P_\Lambda}{P_{\Sigma^0}}, \qquad (6)$$

where P_Λ is the polarization of the Λ's produced in the direct reaction (*a*) and $P_{\Lambda\text{ind}}$ is the polarization of the Λ's produced in the indirect reaction (*b'*). A measurement of (6) is therefore a measurement of the ratio of the Λ to Σ polarizations from which, as we have seen, the Σ - Λ parity can be deduced without ever using the knowledge of the α's.

(B) From the fact that Y^* is in a pure state of isotopic spin $I = 1$, it follows that in reactions (*b*) and (*c*) we have $P_{\Sigma^+} = P_{\Sigma^0}$. As a consequence the measured ratio of the up/down asymmetries in the decays (*a'*) and (*c'*) gives

$$\frac{\alpha_\Lambda P_\Lambda}{\alpha_0 P_{\Sigma^+}} = \frac{\alpha_\Lambda P_\Lambda}{\alpha_0 P_{\Sigma^0}} \left[= \frac{\alpha_\Lambda}{\alpha_0} \left(- \frac{P_\Lambda}{3 P_{\Lambda\text{ind}}} \right) \right]. \qquad (7)$$

P_Λ / P_{Σ^0} being known from the previous experiment, one obtains $\alpha_\Lambda / \alpha_0$ directly.

A few concluding remarks are perhaps necessary. First of all, too much significance should not be attached to the actual numbers given in (3) and (4). The interference effect caused by other channels than the resonating one considered in (1) or (1'), and also the fact that the intermediate state Y^* has an extremely short lifetime ($\sim 10^{-23}$ sec), may bring about substantial corrections. However, it is felt that the difference in sign still survives after corrections and that is the significant piece of information for the Σ - Λ parity. As for the ratio $\alpha_\Lambda / \alpha_0$, its absolute value is already known to be ~ 1 but its sign is particularly important to determine because of its bearing on the proposed theories of weak interactions for nonleptonic decays of strange particles.[7]

It should also be noted that the proposed experiment can provide a check of the internal consistency of the whole scheme. For instance, a necessary condition for the validity of our assumption (I) is that the branching ratio for the cross sections $\sigma(\pi^+ + p \to K^+ + \Sigma^0 + \pi^+)$ and $\sigma(\pi^+ + p \to K^+ + \Sigma^+ + \pi^0)$ be not too far from 1, etc.

In conclusion, it appears that provided conditions (I) and (II) are confirmed by experiment and provided the observed polarizations are large enough,[8] one can get the relative Σ - Λ parity and the sign of $\alpha_\Lambda / \alpha_0$ by measuring only the up/down asymmetries in the hyperon decays (*a'*), (*b''*), and (*c'*).

Whatever the situation turns out to be, the experimental investigation of the reaction considered here will give useful information on the position, width, spin, etc.,[9] of the resonance(s), and can shed some light on the understanding of strange particle interactions.

We are grateful to Dr. V. Glaser for some discussions. Two of us (P.M. and Y.Y.) would like to thank CERN for its hospitality.

*On leave from Faculté des Sciences, Orsay, and Université de Bordeaux, Bordeaux, France.

†On leave from Osaka City University, Osaka, Japan.

[1]Reported by M. L. Good at Tenth Annual Rochester Conference on High-Energy Nuclear Physics, August, 1960 (to be published).

[2]$(b)/(a) = (c)/(a) = 1/4$ if the restricted (or global) symmetry is valid [in which, however, $\Pi(\Lambda) = \Pi(\Sigma)$ is assumed]. Kinematical factors, including the Σ - Λ mass difference, would give $\sim 1/20$ if Y^* is the p_{y_2} pion-hyperon resonance (analogous to the 33 resonance of the π - N system). Nevertheless there is no strong reason to believe such predictions.

[3]For this reason among others the use of a hydrogen bubble chamber seems more suitable.

[4]The situation here is analogous to the one considered in nuclear physics in the decay of the compound nucleus, etc.

[5]Formulas (3) and (4) are special cases of the more general relation,

$$P_\Lambda [P_\Sigma] = \left\{ \begin{matrix} 1 \\ -J/(J+1) \end{matrix} \right\} \times P_{Y^*}$$

$$\text{for } \Pi(\Lambda)[\Pi(\Sigma)] = \left\{ \begin{matrix} (-1)^{J+\frac{1}{2}} \\ (-1)^{J-\frac{1}{2}} \end{matrix} \right\} \Pi(Y^*),$$

where P_{Y^*} is the polarization of Y^* which is of course normal to the plane S.

[6]R. Gatto, Phys. Rev. 109, 610 (1958); G. Feldman and T. Fulton, Nuclear Phys. 8, 106 (1958).

[7]B. d'Espagnat and J. Prentki, Phys. Rev. 114, 1366 (1959); S. Bludman, Phys. Rev. 115, 468 (1959); S. Treiman, Nuovo cimento 15, 916 (1960); A. Pais, Nuovo cimento (to be published).

[8]If $\Pi(\Lambda) = \Pi(\Sigma) = (-1)^{J+\frac{1}{2}} \Pi(Y^*)$ were the case, the experiment would be easiest; otherwise the polarizations of hyperons are smaller and better statistics is of course required. This follows from footnote 5.

[9]The determination of the spin of Y^* can be obtained by standard methods which shall not be discussed here.

HIGH-ENERGY BEHAVIOR OF CROSS SECTIONS IN QUANTUM ELECTRODYNAMICS

K. E. Eriksson and A. Peterman
CERN, Geneva, Switzerland
(Received October 10, 1960)

If one wishes to detect a possible breakdown of quantum electrodynamics at small distances by comparing high-energy scattering experiments with theoretical predictions available to some given order in α, the following question arises: What is the magnitude of the radiative corrections beyond that order? One knows indeed that terms of the type $(\alpha/\pi)^n \ln^{2n}(q^2/m^2)$, where q is the invariant momentum transfer and m the electron rest mass, are likely to occur in a series expansion in α. In other words, one is presented with corrections which are possibly expressed as a series expansion in the effective parameter $(\alpha/\pi) \ln^2(q^2/m^2)$. Such a situation actually obtains in scattering processes of a spin $\frac{1}{2}$ particle by a neutral vector meson field with nonvanishing rest mass, and in quantum electrodynamics in several first order corrections to cross sections, evaluated in the laboratory system.[1] The importance of the possible existence of such $(\alpha/\pi)^n \times \ln^{2n}(q^2/m^2)$ terms is made apparent by considering an experiment,[2] in which $q^2 = 10^6 m^2$, yielding $\ln(q^2/m^2) \cong 14$, so that $\ln^2(q^2/m^2) \cong 200$ would make the convergence of the perturbation expansion very doubtful—to say the least.

We have now investigated in detail the problem, whether the effective expansion parameter is indeed $(\alpha/\pi) \ln^2(q^2/m^2)$, and we conclude that this is not the case but that the series of radiative corrections to scattering cross sections, evaluated in the c.m. system, is rather an expansion in terms of an effective parameter which is at most

$$(\alpha/\pi) \ln^{4/3}(q^2/m^2). \qquad (1)$$

The available first order calculations related to various processes described in the c.m. system[2,3] agree with the above theorem on the maximum power of $\ln(q^2/m^2)$. However, one could not from these first order calculations alone conclude as to whether the maximum power involved is n or $2n-1$, as these are equal for $n=1$. Our theorem provides the means to rule out—among other things—the occurrence of $(\alpha/\pi)^n \ln^{2n-1}(q^2/m^2)$ terms, which could invalidate the meaning of first order calculations due to a breakdown of the expansion.

Our proof is based on a method similar to that of Sudakov.[4] The variables of integration, k_i, in momentum space are first resolved into components parallel and perpendicular to the "plane" determined by the initial and final electron momenta p and p'. It is next shown that the $(2n)$th order Spence functions,[5] to which one is led in evaluating the nth order correction to the elastic scattering cross section, originate from soft-photon contributions exclusively. Cutting off the photon momenta in the infrared can be achieved by forbidding that both components along p and p' are small at the same time.[6] The $(2n)$th order Spence functions thus factorize into bilinear products of nth order Spence functions involving q^2/m^2 and nth order Spence functions involving the infrared cutoff. The latter, as is well known, can be eliminated rigorously in terms of the maximum energy loss ΔE (in the c.m. system), involved in the corresponding inelastic processes with emission of soft real photons and electron pairs, under the condition that ΔE is small compared to the c.m. energies E of the scattered particles.[7]

The nth order Spence functions are asymptotically equal to $\ln^n$ for large arguments. But contributions of the form $\ln^n(E/\Delta E)$ are harmless, because they can be summed in closed form, if $\Delta E/E \ll 1$, i.e., when $\ln(E/\Delta E)$ is large.[8] On the other hand, it just happens that in the case of realistic high-energy experiments, ΔE is not expected to be much smaller than E, so that $\ln(E/\Delta E)$ will amount only to a few units.[2] Therefore, the only large quantity that will occur to any order in α is $(\alpha/\pi) \ln(q^2/m^2)$. The exponent 4/3 in (1) stems from the fact that for corrections involving closed electron loops the analysis is much more complicated, and 4/3 is the upper bound for the exponent that could be derived with a reasonable amount of work. It is very likely, of course, that actually $(\alpha/\pi) \ln(q^2/m^2)$ simply occurs. The methods to prove this are very intricate and would not be justified considering that an expansion in terms of (1) "converges" rapidly enough for energies higher than any energy realizable in the foreseeable future.[9]

The fact that at most only $(\alpha/\pi)^n \ln^{\frac{4}{3}n}(q^2/m^2)$ terms can occur makes it now possible to decide whether or not standard quantum electrodynamics

remains valid at the high energies available nowadays, because it shows that the first order terms of the perturbation expansion are meaningful and reliable. Moreover, for the presently proposed experiments, the calculation of the leading corrections in first order in α to $\sigma_{el}+\sigma_{soft}$ is quite sufficient for the precision needed. Of course, in addition to soft photons and pairs, a large amount of hard photons and pairs may be emitted along the directions of the incoming and outgoing momenta. Thus the cross sections should be written as

$$\sigma=\sigma_{el}+\sigma_{soft}+\sigma_{hard}+\sigma_{hard+soft}. \qquad (2)$$

But the cross section for hard photon and pair emission, σ_{hard}, is very sensitive to the experimental geometry and must be calculated separately for every particular experimental design.[10]

---

[1]L. M. Brown and R. P. Feynman, Phys. Rev. 85, 231 (1952); M. L. G. Redhead, Proc. Roy. Soc. (London) A220, 219 (1953); R. V. Polovin, J. Exptl. Theoret. Phys. (U.S.S.R.) 31, 449 (1956)[translation: Soviet Phys. -JETP 4, 385 (1957)]. G. Furlan and G. Peressutti, Nuovo cimento 15, 817 (1960).

[2]Y. S. Tsai, Nuovo cimento 16, 370 (1960) and Phys. Rev. 120, 269 (1960).

[3]J. Schwinger, Phys. Rev. 76, 790 (1949); H. Suura, Phys. Rev. 99, 1020 (1955); K. Hiida, T. Murota, M. Goto, and M. Sasanuma, Progr. Theoret. Phys. (Kyoto)(to be published). K. E. Eriksson (to be published).

[4]V. V. Sudakov, J. Exptl. Theoret. Phys. (U.S.S.R.) 30, 87 (1956) [translation: Soviet Phys. -JETP 3, 65 (1956)]; see also A. A. Abrikosov, J. Exptl. Theoret. Phys.(U.S.S.R.) 30, 96 (1956) [translation: Soviet Phys.-JETP 3, 71 (1956)].

[5]K. Mitchell, Phil. Mag. 40, 351 (1949); H. F. Sandham, J. London Math. Soc. 24, 83 (1949).

[6]If the perpendicular component is kept finite, one gets contributions which can be neglected (see reference 4).

[7]N. Nakanishi, Progr. Theoret Phys. (Kyoto) 19, 159 (1958).

[8]D. R. Yennie, S. C. Frautschi, and H. Suura (to be published); K. E. Eriksson (to be published).

[9]For instance, for $q=100$ Bev, (1) yields roughly 1/6.

[10]The last term in (2) gives the correction to σ_{hard} due to emission of soft photons and pairs. The result obtained above for $\sigma_{el}+\sigma_{soft}$ applies also for $\sigma_{hard}+\sigma_{hard+soft}$ and thus for the complete cross section.

ABSTRACTS

In this section are printed the abstracts of Articles that have been forwarded to The American Institute of Physics for publication in THE PHYSICAL REVIEW. In quoting information obtained from this section before the appearance of the corresponding Article, reference should be made to "Physical Review (to be published)" rather than to this Journal.

ENERGY-MOMENTUM TENSOR FOR PLANE WAVES. P. A. Sturrock, Microwave Laboratory, W. W. Hansen Laboratories of Physics, Stanford University, Stanford, California (Received August 19, 1960).

A general form is established for plane waves propagating in a homogeneous medium, the field equations of which are derivable from a quadratic Lagrangian function. Energy density and momentum density are proportional to frequency and the wave vector, the coefficient of proportionality being "action density." Energy flow and momentum flow are related to energy density and momentum density by the group velocity. The relation between momentum density and the wave vector is valid even in a nonlinear system. For a wave packet, one finds that the total energy is related to frequency and the total momentum to the wave vector by the total action of the packet, in close analogy with corresponding relations of quantum mechanics.

NUCLEAR MAGNETIC RESONANCE OF Xe^{129} IN NATURAL XENON. R. L. Streever* and H. Y. Carr, Department of Physics, Rutgers University, New Brunswick, New Jersey (Received August 3, 1960).

The spin-lattice relaxation time T_1 of Xe^{129} has been measured as a function of temperature in the liquid and as a function of pressure in the gas. A strong shift ΔH in the external field required for resonance at constant frequency but varying sample density ρ has been discovered. As the sample density increases in the region above 48 atm, ΔH decreases linearly at the rate of 3.45 milligauss per amagat (density at standard conditions) in a field of 8060 gauss. In the liquid the temperature dependence of the product of T_1 and ρ can be described by an activation energy of 0.7 ± 0.1 kcal/mole. In the gas at room temperature between 48 and 73 atm, T_1 varies as $\rho^{-2.1 \pm 0.4}$. The largest value of T_1 observed was 2600 ± 600 sec for a gas sample at 48 atm, and the shortest value was 57 ± 2 sec in the liquid at -101°C. The experimental values of T_1 have been compared with theoretical predictions in two limiting cases, the rare gas and the dense liquid. In both cases the experimental values, although larger than previously reported values, are still two to three orders of magnitude smaller than predicted from an intermolecular nuclear magnetic dipole interaction. The relaxation time was found to be independent of field. Implications of our data for determining the relaxation mechanism are discussed. It is suggested that the relaxation may be caused by a fluctuating magnetic field at the nucleus resulting from the motion of nonsymmetrical electronic charge distributions during collisions.

*Now at National Bureau of Standards, Washington, D. C.

MEASUREMENT OF THE g FACTOR OF FREE, HIGH-ENERGY ELECTRONS. A. A. Schupp,* R. W. Pidd,* and H. R. Crane, Harrison M. Randall Laboratory of Physics, The University of Michigan, Ann Arbor, Michigan (Received August 17, 1960).

100-kev electrons in 0.1-μsec bunches are sent into a gold foil. The part of the electron bunch which is scattered at right angles, and which, consequently, is partially polarized, is trapped in a magnetic field and held for a measured length of time (up to 300 μsec). The bunch is then released from the trap and allowed to strike a second gold foil. Counters receive the electrons scattered at plus and minus approximately 90°. The cycle is repeated 1000 times per sec. The asymmetry in intensity in the two directions depends upon the final direction of polarization. A plot of the intensity asymmetry vs trapping duration is a cosine curve, whose frequency is the difference between the orbital frequency and the spin precession frequency. This is related to the g factor as follows: $\omega_D m_e c/Be = a$, where g is $2(1+a)$. Thus the "anomaly" a is measured directly. The determination of B presents some difficulty because the field must be slightly nonuniform in order to trap the electrons. The spatial variation in B from the center of the trap to the ends is only 0.3%, and the time average of B which applies to the trapped electrons is evalu-

ated to 0.1%. Measurements made at other electron energies, down to 50 kev, showed a slight dependence of a upon energy. The dependence is attributed to electrostatic charges on the surfaces in the trapping region. The final standard error quoted is, however, purposely made large enough so that the variation of a with energy is bracketted. The result is $a = 0.0011609 \pm 0.0000024$.

*Now at General Atomic Corporation, La Jolla, California.

SELF-DIFFUSION IN LIQUID He^3. Daniel Hone, University of Illinois, Urbana, Illinois (Received August 19, 1960).

The Landau model of a Fermi liquid is employed to obtain an expression for the coefficient of self-diffusion, D, in liquid He^3. It is found that $D = A/T^2$, where $A \approx 2 \times 10^{-6}$ cm^2 sec^{-1} degree^2, and T is the temperature in degrees Kelvin. As this temperature dependence differs from that experimentally observed ($T^{-3/2}$), although the order of magnitude of the theoretical prediction agrees well with experiment, the possible effect of the 1% He^4 impurity known to be present is investigated; it is found that the diffusion coefficient is essentially unaffected by the impurity (a result also obtained experimentally). It is estimated that the Landau model is applicable only well below 0.05°K. As even the most recent experiments have been carried out only down to 0.03°K, it is concluded that the transport properties of He^3 should be investigated experimentally at lower temperatures in order to check the validity of the theory.

EFFECT OF HIGH PRESSURE ON ELECTRICAL PROPERTIES OF NiO, CoO, CuO, and Cu_2O. A. P. Young, W. B. Wilson, and C. M. Schwartz, Battelle Memorial Institute, Columbus, Ohio (Received May 26, 1960; revised manuscript received September 6, 1960).

The effect of pressure on electrical resistance and Seebeck coefficient at or near room temperature in NiO, CoO, CuO, and Cu_2O has been determined. Equations relating the Seebeck coefficient to hole concentration have been used to calculate the effect of pressure on hole mobility. In all materials examined, hole mobility was decreased by pressures to 60 000 atm. It has been proposed that NiO charge transport occurs by the motion of holes trapped at local sites by polarization of the surrounding lattice. The effect of pressure on the diffusion of self-trapped holes has been considered. Motion of self-trapped holes in an ionic crystal and of vacancies in a metal may be similar to the extent that the motion of either probably involves cooperative movements of surrounding ions or atoms. Some inward relaxation probably occurs around either a hole trapped at a local site in an ionic crystal or around a vacancy in a metal. In either case pressure would be expected to decrease the jump frequency for motion of the defect. It is proposed that in NiO, CoO, and CuO, the decreased hole mobility with pressure was due to a decrease in diffusion rate of self-trapped holes. The explanation for pressure effects in Cu_2O may be more complicated since Cu_2O is generally regarded as a wide-band semiconductor.

NEUTRON DIFFRACTION INVESTIGATION OF MAGNETIC ORDERING IN THE TRIFLUORIDES OF 4d TRANSITION ELEMENTS. M. K. Wilkinson, E. O. Wollan, H. R. Child, and J. W. Cable, Oak Ridge National Laboratory, Oak Ridge, Tennessee (Received August 18, 1960).

MoF_3 becomes antiferromagnetic below 185°K with a spin-only magnetic moment corresponding to $S = 3/2$ and a magnetic structure which can be correlated with coupling rules applicable to the iron-group trifluorides. These results, together with the absence of observable magnetic neutron scattering from PdF_3 and RuF_3, suggest that Hund's rule does not apply to ions in the 4d-transition series.

HYPERFINE STRUCTURE OF Fe^{57} IN PARAMAGNETIC AND ANTIFERROMAGNETIC FeF_2 FROM THE MÖSSBAUER EFFECT. G. K. Wertheim, Bell Telephone Laboratories, Murray Hill, New Jersey (Received August 25, 1960).

Measurements of the gamma-ray resonant absorption in oriented slabs of FeF_2 have been used to determine the magnitude and direction of the magnetic field at the iron nucleus in the antiferromagnetic state (3.40×10^5 oe at 0°K) and the quadrupole coupling in the paramagnetic state (31.2 Mc/sec) of this material. The observed electric and magnetic hfs in the antiferromagnetic state is interpretable in terms of an

asymmetric electric field gradient tensor with its major axis perpendicular to the c axis, an asymmetry parameter of 0.33, and a quadrupole coupling of 30.3 Mc/sec at 45°K.

MAGNETIC STUDIES ON SINGLE-CRYSTAL CHROME POTASSIUM ALUM BELOW 1° KELVIN. A. C. Thorsen,* Rice University, Houston, Texas (Received August 29, 1960).

The magnetic susceptibility of a spherically shaped single crystal of chrome potassium alum has been measured as a function of entropy and applied external field along the [100], [110], and [111] directions in the crystal at temperatures below 0.1°K. Zero-field measurements of the static susceptibility were made with a moving-coil apparatus and longitudinal field measurements were made using the conventional ballistic bridge method. A ballistic galvanometer with period 4.6 seconds was used in both circuits. Drop coil measurements indicate no long-time effects in the magnetization and show no appreciable difference from the susceptibility measured by the ballistic method. The isentropic susceptibility measured in fields up to 300 gauss indicates definite anisotropy below the Néel point in fields from 50 to 300 gauss.

*Now at Atomics International, Canoga Park, California.

NUCLEAR MAGNETIC RESONANCE SPECTRUM OF Co^{59} IN METALLIC COBALT POWDERS. R. Street, Physics Department, Monash University, Victoria, Australia, and D. S. Rodbell and W. L. Roth, General Electric Research Laboratory, Schenectady, New York (Received August 23, 1960).

The nuclear magnetic resonance spectrum of Co^{59} in metallic powders is presented. This spectrum contains three lines in addition to the already well-known line of Co^{59} in face-centered cubic cobalt (213.1 Mc/sec at 25°C). The other lines are higher in frequency; the highest is located 10 Mc/sec above the fcc resonance and is much less intense than the fcc. This highest lying resonance is identified to be due to Co^{59} nuclei in hexagonal close-packed cobalt, and we qualitatively account for the lower intensity by examining the effect on the resonance of the nuclear quadrupole moment in a noncubic environment.

ELECTROLUMINESCENCE OF ZINC SULFIDE SINGLE CRYSTALS. I. T. Steinberger, V. Bar, and E. Alexander, Department of Physics, The Hebrew University, Jerusalem, Israel (Received August 3, 1960).

In a series of experiments designed to distinguish between ionization and recombination processes during electroluminescence (EL), rectangular voltage pulses were applied to single crystals of zinc sulfide. During the "on" period, the emission gradually increased to a stationary level. Removal of the voltage resulted in a burst of emission, which decayed slowly. This behavior is explained by the assumption of three field-dependent processes, namely: (a) ionization of centers in barrier regions; (b) sweeping out of the liberated electrons from the vicinity of the centers; (c) tunnelling of electrons into the barrier regions. It was found that for a considerable voltage range the product of the light-sum (measured during the "off" period) by the current was proportional to the stationary emission level during the "on" period. This proportionality strongly supports the model suggested.

In many cases the current was found to be dependent more strongly on the voltage than the light sum. This result favors an ionization mechanism which is independent of the current.

The model suggests furthermore an alternative explanation for the Neumark effect, i.e., the enhancement of the thermal glow by electric fields. The explanation does not involve an impact-ionization mechanism.

HEAT CAPACITY OF FERROMAGNETIC SUPERCONDUCTORS. Norman E. Phillips, Department of Chemistry and Lawrence Radiation Laboratory, University of California, Berkeley, California, and B. T. Matthias, Bell Telephone Laboratories, Murray Hill, New Jersey (Received August 15, 1960).

Heat capacity measurements on two samples from each of the systems $La_{1-x}Gd_x$ and $Y_{1-x}Gd_xOs_2$ show features which are correlated with the reported existence of both ferromagnetic and superconducting transitions. For one sample the measurements cover a wide enough temperature range to show that the entropy associated with the ordering of the gadolinium spins is the xR ln8 expected for complete order. The heat capacities of the other samples are

consistent with complete ordering. Superconducting transitions have been observed both above and below the maximum in the heat capacity associated with the spin ordering. The entropy differences between the normal and superconducting states show that superconductivity is not confined to small volume elements but probably extends throughout the sample.

NUCLEAR MAGNETIC RESONANCE AND MAGNETIC ORDERING IN NiF_2. R. G. Shulman, Bell Telephone Laboratories, Murray Hill, New Jersey, and Fysisk-Kemisk Institut, University of Copenhagen, Copenhagen, Denmark (Received August 30, 1960).

Measurements of the nuclear magnetic resonance of the F^{19} nucleus in single crystals of NiF_2 have been made at temperatures between 4.2°K and 298°K. In the paramagnetic state at 298°K, for arbitrary directions of $\vec{H}_0$ two resonances were observed, while for $\vec{H}_0$ in a (100) plane only one resonance was observed as expected from the crystal symmetry. The shift of the resonances from the normal resonance field ω/γ_N allows one to calculate three independent parameters of the hyperfine interaction between the F^{19} nuclei and the magnetic electrons. In conjunction with measurements made in the antiferromagnetic state, it was possible to determine the individual components of the hyperfine interaction in units of 10^{-4} cm^{-1} as $A_s^{I} = 36.4 \pm 1.8$, $A_s^{II} = 42.1 \pm 2.1$, $A_\sigma^{I} = 9.1 \pm 0.9$, and $A_\sigma^{II} = 9.9 \pm 0.9$. Superscripts refer to the two different bonds with Ni^{++} and subscripts s and σ refer to isotropic and anisotropic contributions. From these we calculate that the fractions of unpaired spin in the corresponding fluoride ion s and p_σ orbitals are $f_s^{I} = (0.46 \pm 0.02)\%$, $f_s^{II} = (0.54 \pm 0.03)\%$, $f_\sigma^{I} = (4.1 \pm 0.4)\%$, and $f_\sigma^{II} = (4.5 \pm 0.4)\%$. Since geometrical considerations almost completely forbid magnetic p_π interactions in NiF_2, there is a negligible cancellation of p_σ interactions by the p_π so that, unlike MnF_2 and FeF_2, the admixture of magnetic electrons into fluoride ion orbitals is almost completely determined.

At temperatures just above the antiferromagnetic transition $T_N = 73.2$°K the resonance shifts with $\vec{H}_0$ in the (001) plane change rapidly with temperature. Between 75.7°K and T_N the susceptibility of one sublattice becomes negative while the other remains positive. This has been correlated with the sublattice susceptibility derived by Moriya from the spin Hamiltonian $\mathcal{H} = g\beta H + DS_z^2 + E(S_x^2 - S_y^2)$. By fitting the theoretical susceptibility we have determined the sign of E in this Hamiltonian.

Below 73.2° the nuclear resonances are consistent with Moriya's model in which the spins are antiparallel along [100] and tipped ~1.3° towards [010]. Ericson's description of the magnetic ordering is shown to be incorrect. In the antiferromagnetic state the F^{19} resonance in the domains broadens as $\vec{H}_0$ is lowered below 5000 gauss.

ELASTIC CONSTANTS OF CsBr FROM 4.2°K TO 300°K. Billy J. Marshall, The Rice University, Houston, Texas (Received August 22, 1960).

Measurements of the elastic constants from 4.2°K to 300°K have been made on single crystals of cesium bromide. The values of the elastic constants at 4.2°K are $c_{11} = 3.350 \pm 0.8\%$, $c_{12} = 1.025 \pm 10\%$, and $c_{44} = 1.002 \pm 0.8\%$ in units of 10^{11} dynes/cm^2. The Debye temperature (θ_0) at 0°K as calculated from the elastic constants is 149.0°K ± 2°K. The lattice energy at 0°K is computed to be $U_0 = 147.6$ kcal/mole.

VOLUME-CONTROLLED, TWO-CARRIER CURRENTS IN SOLIDS: THE INJECTED PLASMA CASE. Murray A. Lampert and A. Rose, RCA Laboratories, Princeton, New Jersey (Received August 12, 1960).

Double injection into semiconductors and insulators is studied under conditions where the injected electrons and holes are free (injected plasma), the current is volume-controlled (i.e., determined by distributed space charge), and the current is field-driven (diffusion negligible). The major results are, assuming a one-dimensional geometry and carrier lifetime independent of injection level, for extrinsic semiconductors, (i): an extended voltage region over which $J \propto V^2$ (J = current density and V = voltage), and (ii) depression of the current, at fixed voltage, in the square-law region through increase in the number of thermal minority carriers, $J \propto |n_T - p_T|$, with n_T and p_T the thermal-equilibrium densities of electrons and holes, respectively. This unusual behavior is shown to be a direct consequence of recombination kinetic requirements.

For insulators, assuming trapping is negligible, $J \propto V^3$. A rigorous solution is obtained for the constant-lifetime problem, valid for both semiconductors and trap-free insulators. This solution furnishes a good approximation also for variable-lifetime cases, e.g., bimolecular recombination kinetics.

CURRENT-VOLTAGE CHARACTERISTICS OF FORWARD BIASED LONG p-i-n STRUCTURES. R. D. Larrabee, RCA Laboratories, Princeton, New Jersey (Received August 12, 1960).

The current-voltage characteristics have been observed in several germanium p-i-n structures in which the n side was biased negative and the p side positive so as to cause a double injection of electrons and holes into the structure. The middle i section was constructed of good quality germanium (approximately 2×10^{13} donors/cm^3) and was many minority carrier diffusion lengths long. The observed I-V characteristics display a low-field region in which the current is proportional to the voltage, followed by a higher-field region in which the current is proportional to the square of the voltage. In the square-law region, the current is a function of the difference, rather than the sum, of the thermal densities of the electrons and holes. These observations lend experimental support to the basic theories of Lampert and Rose regarding volume-controlled double injection into a semiconductor.

VALENCE BAND EMISSION SPECTRA OF IRON, COBALT, AND NICKEL. D. H. Tomboulian and D. E. Bedo, Cornell University, Ithaca, New York (Received August 25, 1960).

The paper reports results on the shapes of the $M_{2,3}$ emission bands (valence $-3p$) of Fe, Co, and Ni. The relative intensity distributions were arrived at by removing the underlying background contribution in accordance with the predictions made available from recent investigations dealing with the behavior of the soft x-ray bremsstrahlung intensity. In the spectrum of Fe the peak of the composite $M_{2,3}$ band falls at 51.3 ev. The peaks in the Co and Ni spectra are located at 57.8 ev and 64.8 ev, respectively. The high-energy limits are estimated to fall at 56.5 ev, 61.4 ev, and 68.9 ev for Fe, Co, and Ni, respectively. The over-all composite bandwidths in ev in the order of metals just cited are found to be 14.5, 10.8, and 8.9. These estimates include the low-energy tail belonging to the individual M_3 spectral bands. An attempt was made to resolve the Fe $M_{2,3}$ complex band into individual M_2 and M_3 bands. In this process the inner levels were regarded as sharp, but the influence of Auger reorganization upon the relative band intensities was taken into account. For Fe, this process gives an individual bandwidth of 8.0 ev. The results of the present observations are compared with other determinations of band contours. The various measurements are in agreement as to the location of the peak energy but there are differences in the intensity profiles and bandwidths.

ISOTOPE EFFECT IN SUPERCONDUCTING LEAD. R. W. Shaw,* D. E. Mapother, and D. C. Hopkins, Physics Department, University of Illinois, Urbana, Illinois (Received July 18, 1960).

The present work is a continuation of earlier measurements of the difference in critical fields of superconducting Pb specimens with various isotopic masses. The isotope samples have been repurified and the low-temperature behavior is now more fully understood. The results near T_C are consistent with the relation $T_C = \text{const}\times M^p$, where M is the average isotopic mass, and yield a value $p = -0.478 \pm 0.014$. The measurements at lower temperatures confirm the similarity principle to within approximately 0.1% and indicate that γ, the coefficient in the normal electronic specific heat, is independent of isotopic mass to a similar accuracy.

*Present address: Physics Department, Rensselaer Polytechnic Institute, Troy, New York.

CARRIER LIFETIME IN INDIUM ANTIMONIDE. R. A. Laff* and H. Y. Fan, Department of Physics, Purdue University, Lafayette, Indiana (Received August 22, 1960).

The recombination of excess electron-hole pairs in indium antimonide has been studied in the temperature range 200°K-15°K, where it is controlled by localized centers. Minority carrier trapping is found in extrinsic p-type material. The lifetimes of electrons and holes obtained from photoconductivity and photoelectromagnetic

effect data on n- and p-type samples lead to a model for the recombination, consisting of a donor center having two energy levels in the forbidden gap, at 0.055 and 0.12 ev above the valence band. The capture rates for holes and electrons have been determined for the center in each of the two charge states. In p-type material, the chemical acceptors are in statistical equilibrium with the free holes in the valence band. When holes freeze out onto acceptor centers ($T < 60°K$), an increase of free holes due to photoexcitation leads to a corresponding increase in the hole concentration on the acceptors. This effect of majority carrier trapping reduces the rise of hole lifetime with decreasing hole concentration. In order to determine the nature of the recombination centers, different treatments are used to introduce additional centers. It is found that bombardment with 4.5-Mev electrons produces additional centers having the same recombination properties as the original centers. The result indicates that the recombination centers have the nature of structural defects rather than chemical impurities.

*Now at IBM Research Laboratories, Poughkeepsie, New York.

NUCLEAR MAGNETIC RESONANCE OF Ni^{61} IN METALLIC NICKEL. L. J. Bruner, J. I. Budnick, and R. J. Blume, International Business Machines Watson Research Laboratory, Columbia University, New York, New York (Received August 29, 1960).

The nuclear magnetic resonance of Ni^{61} in unenriched metallic nickel has been observed. The results provide the first experimental measure of the internal field at the nucleus in nickel. The resonance occurs at a frequency of 26.02 Mc/sec at room temperature, yielding an estimate of 170 kilogauss for the internal field.

MAGNETIC FIELD DEPENDENCE OF ENERGY GAP IN SUPERCONDUCTORS. K. K. Gupta* and V. S. Mathur, The Enrico Fermi Institute for Nuclear Studies and the Department of Physics, The University of Chicago, Chicago, Illinois (Received July 20, 1960).

The dependence of energy gap in superconductors on static magnetic fields has been derived in a gauge-invariant way from the theory of Bardeen, Cooper, and Schrieffer. It has been shown that the gap width decreases with magnetic field approaching the critical value. Optimum conditions have been discussed for the observation of such an effect. The decrease in gap width has been calculated for two superconductors, Al and Sn, and it has been shown that for film thickness between 10^{-4} to 10^{-5} cm, the effect can be large enough to be observable.

*Present address: Tata Institute for Fundamental Research, Bombay, India.

ELECTRONIC STRUCTURE OF THE CENTERS IN ZnS. Joseph L. Birman, University of Pennsylvania, Philadelphia, Pennsylvania, and General Telephone and Electronics Research Laboratories, Bayside, New York (Received August 30, 1960).

A model of the common sulfide luminescent centers is proposed. The mutual perturbation of crystal eigenstates and transition metal (activator) "d" eigenstates is assumed to give rise to the excited and unexcited eigenstates of the center. For substitutional Cu^+ (d^{10}) in zincblende, zeroth order crystal field theory predicts that two sets of occupied center ground-state levels (T_2 and E) originating from d^{10} will exist. Additional level splittings result from (a) the spin-orbit effect, and (b) axial crystal field splittings in wurtzite. Experiments on visible and infrared excitation and emission are used to make tentative assignments of magnitude of level splittings.

MAGNETIC PROPERTIES OF $KMnF_3$. I. CRYSTALLOGRAPHIC STUDIES. Olof Beckman,* University of California, Berkeley, California, and Kerro Knox, Bell Telephone Laboratories, Murray Hill, New Jersey (Received August 22, 1960).

The lattice parameters for $KMnF_3$ have been determined by means of an x-ray rotation camera designed for temperatures down to 15°K. The cubic room temperature perovskite structure transforms at 184°K to an orthorhombic phase with D_{2h}^{16} - $Pbnm$ as the most probable space group with a unit cell containing 4 formula units; it has a tetragonal pseudocell with $c/a > 1$ in which the fluorine octahedra about the manganese remain essentially regular but tilt relative to the crystal axes. At 84°K, just below the

Néel temperature of 88°K, the pure antiferromagnetic also has a tetragonal pseudocell, but with $c/a < 1$ and the still essentially regular octahedra rotated as well as twisted. Below a second magnetic transition at 81.5°, the 65° structure shows in addition a significant distortion of the regularity of the octahedra.

*On leave from Uppsala University, Uppsala, Sweden.

OPTICAL ABSORPTION OF CUPROUS OXIDE. Philip W. Baumeister,* Department of Physics, University of California, Berkeley, California (Received July 19, 1960).

The relative optical absorption coefficient α of polycrystalline slabs of cuprous oxide was measured at 295°K, 77°K, and 4.2°K. At 4.2°K, α is proportional to $(\sigma - E_0)^{1/2}$ for 16 510 $\text{cm}^{-1} \leq \sigma \leq 16\,900\ \text{cm}^{-1}$, where σ is the wave number. At 77°K an additional component appears, so that $\alpha = \alpha_1 + \alpha_2$, with $\alpha_1 \propto (\sigma - E_1)^{1/2}$ and $\alpha_2 \propto (\sigma - E_2)^{1/2}$. This is attributed to indirect transitions to exciton levels, in agreement with a theory by Elliott. The ratio of the integrated absorption coefficient of the first two exciton lines, after corrections for the background were applied, is also in satisfactory agreement with the Elliott theory.

*Present address: Institute of Optics, University of Rochester, Rochester, New York.

ELECTROMAGNETIC PROPERTIES OF INSULATORS. II. Vinay Ambegaokar,* Carnegie Institute of Technology and Westinghouse Research Laboratories, Pittsburgh, Pennsylvania (Received August 31, 1960).

This paper is a continuation of an earlier study, from a many-particle point of view, of the electromagnetic properties of insulators. Here the system of an insulator and one electron is treated. The Coulomb interactions between all the electrons in the system are allowed for to all orders of perturbation theory. The true effective mass, m^*, of the extra particle is defined as the curvature in wave vector space of the energy surface connecting the ground state and the low-lying excited states of the interacting system. The central result then obtained is that the response of the system to long-wavelength, low-frequency electric fields is exactly that of a free electron of mass m^* moving in a medium characterized by the dielectric constant of the perfect insulator. The energy levels of the system in a static magnetic field are also discussed. An alternative derivation of a single-particle effective-mass equation, previously obtained by Klein, is given. The eigenvalues of this equation are under certain conditions the energy levels of the interacting system in a magnetic field. In an Appendix a Kramers-Kronig relation connecting the difference in optical absorption of the present system and the perfect insulator with m^* is derived. These results indicate that the usual effective-mass theory of semiconductors of low carrier concentration includes the effects of the electron-electron interactions to an excellent approximation.

*Present address: Institute for Theoretical Physics, Copenhagen, Denmark.

PRECISE MEASUREMENT OF THE MICROWAVE ABSORPTION FREQUENCIES OF THE OXYGEN MOLECULE AND THE VELOCITY OF LIGHT. R. W. Zimmerer and M. Mizushima, Department of Physics, University of Colorado, Boulder, Colorado (Received January 22, 1960; revised manuscript received September 26, 1960.

Ten microwave absorption frequencies of the oxygen molecule in the 60-kMc/sec region have been measured with an accuracy of about 10 kc/sec. The result is interpreted by successfully refining the existing theory. Comparing the resultant value of the rotational constant B_0 with the value obtained in ultraviolet spectra, the velocity of light is calculated to be 299 772 ± 12 km/sec.

NUCLEON TRANSFER REACTIONS IN GRAZING COLLISIONS OF HEAVY IONS. Richard Kaufmann and Richard Wolfgang, Department of Chemistry, Yale University, New Haven, Connecticut (Received August 30, 1960).

Reactions in which several nucleons are transferred between complex nuclei have been studied by measurement of angular distributions and excitation functions of the recoiling projectile residues. The results show that multinucleon transfer does not proceed either through a compound nucleus or through a mechanism in which the Coulomb barrier is not penetrated (such as

the tunneling mechanism for single-nucleon transfer). Instead, the data indicate the existence of a "grazing contact" mechanism. In such a grazing reaction, it appears that a high-energy projectile, though deflected by the Coulomb barrier, still penetrates the region of nuclear binding of the target. It moves along the surface of the target, with the zone of contact between the nuclei being frictionally excited and thus preventing formation of a compound nucleus. The system separates after half a rotation, or less, because the repulsive Coulombic and centrifugal forces exceed the nuclear binding force. Depending on the mode of separation, such grazing contact may result in nucleon transfer, inelastic scattering, or breakup of the projectile. At energies well above the Coulomb barrier, such grazing processes appear to represent an important fraction of the geometric cross section.

SINGLE-NUCLEON TRANSFER REACTIONS OF F^{19}, O^{16}, N^{14}, AND C^{12}. Richard Kaufmann and Richard Wolfgang, Department of Chemistry, Yale University, New Haven, Connecticut (Received August 30, 1960).

Results on the angular distribution of single-neutron stripping products are presented. Beams of F^{19}, O^{16}, N^{14}, and C^{12} having an energy of 10 Mev per nucleon, and beams of O^{16} at lower energies were used in conjunction with a rhodium target. The relative contribution of tunneling and grazing transfer processes is discussed. The form of the angular distributions of products originating from the tunneling mechanism is very similar in all systems, although the magnitude of the F^{19} cross section is unexpectedly large. The cutoff distance for closest approach in a tunneling event is found to correspond to the cutoff for elastic scattering.

HIGH-ENERGY ALPHA PARTICLES AND TRITONS FROM THE SPONTANEOUS FISSION OF CALIFORNIUM-252. James C. Watson, Yale University, New Haven, Connecticut (Received August 16, 1960).

The energy spectra of alpha particles and tritons emitted in the spontaneous fission of californium-252 have been measured using an $E-dE/dx$ cesium iodide scintillator–proportional counter detector. The alpha-particle energy spectrum peaks at 16 Mev, with a full width at half maximum of about 15 Mev. The tritons peak at about 8 Mev, with a half-width of 7 Mev. One alpha particle is observed per 345 ± 20 fission events, one triton per 4500 ± 900 fission events.

LIFETIME OF THE FIRST EXCITED STATE OF N^{14}. C. P. Swann, V. K. Rasmussen, and F. R. Metzger, Bartol Research Foundation of the Franklin Institute, Swarthmore, Pennsylvania (Received August 26, 1960).

The mean life of the first excited state of N^{14} has been measured by nuclear resonant scattering. The $N^{14}(p,p')$ reaction with an N^{14}-enriched gaseous ammonia target was used as the source of Doppler-broadened γ radiation. The value of $(7.3\pm1.8)\times10^{-14}$ sec obtained is a factor of two longer than theoretical predictions based on the wave functions used to explain the anomalously slow C^{14} β decay.

NUCLEAR SPINS OF THULIUM-166 AND 167. J. C. Walker and D. L. Harris, Palmer Physical Laboratory, Princeton University, Princeton, New Jersey (Received August 8, 1960).

The spins of 7.7-hour thulium-166 and 9.6-day thulium-167 have been measured by the atomic-beam magnetic resonance method. Spin values are Tm^{166}, $I=2$; Tm^{167}, $I=1/2$.

COULOMB EXCITATION OF SECOND 2^+ STATES IN EVEN-EVEN MEDIUM-WEIGHT NUCLEI. P. H. Stelson and F. K. McGowan, Oak Ridge National Laboratory, Oak Ridge, Tennessee (Received August 22, 1960).

The location of a second 2^+ state has been found for thirteen even-even medium-weight nuclei by means of Coulomb excitation produced by 8-, 9-, and 10-Mev α particles. The relatively weak excitation of these states is detected by a coincident measurement of the cascade gamma rays. From the observed gamma-ray yields, information is obtained on the $B(E2)$'s for the crossover transitions. The crossover $B(E2)$'s exhibit some uniformity and are all rather weak, being about single-particle value or a little less. For some nuclei the cascades/

crossovers ratio for the second 2^+ state is known from other work and it is then possible to extract the $B(E2)$ for the upper cascade transition. These upper cascade $B(E2)$'s exhibit enhancements comparable to those for the lower cascade transitions. Evidence is obtained for the "double $E2$" Coulomb excitation of the 4^+ state in Cd^{114} and this requires an enhanced 4–2 $B(E2)$. In general, the measurements reported support a collective model interpretation, but it is as yet difficult to draw conclusions concerning the shape of the collective potential energy surface governing this motion.

TRITIUM DECAY ENERGY. W. L. Pillinger, Savannah River Laboratory, E. I. du Pont de Nemours and Company, Aiken, South Carolina, and J. J. Hentges and J. A. Blair, Savannah River Plant, E. I. du Pont de Nemours and Company, Aiken, South Carolina (Received June 23, 1960; revised manuscript received September 6, 1960).

The heat output of tritium has been determined by calorimetry as 0.3240 ± 0.0009 watt/gram. This value is about 1 to 4% higher than those previously reported. If the half-life of tritium is 12.43 ± 0.04 years, then its average beta energy is 5.73 ± 0.03 kev.

EXCITATION FUNCTIONS FOR INELASTIC SCATTERING REACTIONS OF CADMIUM-111 AND INDIUM-115. Norbert T. Porile, Chemistry Department, Brookhaven National Laboratory, Upton, New York (Received August 4, 1960; revised manuscript received September 15, 1960).

Excitation functions have been measured for the formation of Cd^{111m} and In^{115m} in the bombardment of Cd^{111} and In^{115}, respectively, with 6-10 Mev protons, 10-20 Mev deuterons, and 15-40 Mev alpha particles. The excitation function for the $In^{115}(\alpha, \alpha n)In^{114m}$ reaction has also been obtained. All the excitation functions increase monotonically with energy. The cross sections for the formation of In^{115m} at the highest bombarding energies are 1.5 mb, 44 mb, and 5.9 mb, for the proton-, deuteron-, and alpha-induced reactions, respectively. The corresponding cross sections for the formation of Cd^{111m} are 2-3 times larger. The results have been compared with the predictions of the statistical theory. The only definite conclusion can be drawn in the case of the $(\alpha, \alpha\gamma)$ reaction where it is shown that an evaporation mechanism cannot account for the measured cross sections at bombarding energies above 25 Mev. The contribution of Coulomb excitation to the observed yields has been calculated. It is found that this process contributes substantially to the $(\alpha, \alpha\gamma)$ and $(p, p\gamma)$ reactions, particularly at low bombarding energies.

TRIPARTITION IN THE SPONTANEOUS-FISSION DECAY OF Cf^{252}. M. Luis Muga, Harry R. Bowman, and Stanley G. Thompson, Lawrence Radiation Laboratory, University of California, Berkeley, California (Received August 29, 1960).

The long-range alpha particles associated with the spontaneous fission decay of californium-252 have been studied by means of nuclear-emulsion techniques. The alpha-particle energy spectrum was found to peak at about 19 Mev with a half-width of 10 Mev, and the preferential angle of emission was found to be slightly less than 90 deg with respect to the light fission fragment. These results support the view that alpha emission occurs at the time of scission and that the direction is determined by the extent of electrostatic repulsion by the fragments. A trend toward a more nearly symmetric mass division in fission accompanied by alpha emission is indicated. The frequency of occurrence of the long-range alpha particles was observed to be 1 in $415 \pm 10\%$ binary fissions.

Ternary events consisting of two heavy fragments and one light fragment of short range were observed, but the frequency with which these events occur was not measured. A parallel search was made for ternary-fission events in which fragmentation into comparable masses occurs.

POSSIBILITY OF A STRIPPING MECHANISM IN TRANSFORMATIONS INDUCED BY LITHIUM IONS. George C. Morrison, The Enrico Fermi Institute for Nuclear Studies, The University of Chicago, Chicago, Illinois (Received July 25, 1960; revised manuscript received September 26, 1960).

Angular distributions of the reaction $Li^7(Li^6, d)B^{11}$ leading to the ground state and first three excited states of B^{11} and the reaction $Li^6(Li^7, t)B^{10}$ leading to the ground state and first excited state of

B^{10} have been studied at an incident energy of 2.1 Mev. The principal features of the observed distributions are their asymmetry about 90° and slow variation of cross section with angle. The results suggest that the reactions proceed at least in part by a stripping mechanism with the capture of the alpha-particle core of the lithium projectile. The importance of this mechanism to the experimental investigation of the cluster model is indicated.

BINDING ENERGY OF THE DEUTERON MEASURED WITH A BENT-CRYSTAL SPECTROMETER. Raymond W. Jewell, Jr., and Walter John, Lawrence Radiation Laboratory, University of California, Livermore, California (Received August 26, 1960).

The binding energy of the deuteron has been determined by measuring the energy of the neutron-proton capture gamma ray with a 2-meter bent-quartz crystal spectrometer in the Cauchois geometry. A polyethylene target in the through-tube of a reactor supplied the n-p capture gamma rays. The 411.77-kev gamma ray of Hg^{198} and the annihilation radiation were used to calibrate the spectrometer. The average of the results of four plates gives 2.225 ±0.003 Mev for the binding energy of the deuteron.

DIFFERENTIAL CROSS SECTIONS OF THE $Be^9(Li^6,\alpha)B^{11}$ REACTION. J. J. Leigh and J. M. Blair, School of Physics, University of Minnesota, Minneapolis, Minnesota (Received August 24, 1960).

The differential cross sections of the $Be^9(Li^6,\alpha)B^{11}$ reaction have been measured as a function of energy and angle. The α particles leaving the B^{11} in the ground state, α_0, in the first excited state, α_1, and in the second and third excited states, $\alpha_2+\alpha_3$, were observed at 10° intervals from 10° to 160° (lab system) at Li^6 energies of 3.00, 3.25, and 3.50 Mev, and at 20°, 60°, 90°, 120°, and 160° (c.m. system) at Li^6 energies of 2.00, 2.50, 3.75, and 4.00 Mev. The angular distributions of the α_0 and α_1 groups are asymmetric about 90° c.m. Relative maxima occur at both large and small angles for each of the α-particle groups, with the yields at large angles being comparable to those at small angles. In all cases the angular distribution varies slowly with bombarding energy and the yields at each angle increase monotonically with increasing energy. At 3.50 Mev the total cross sections are 9.7 ± 3.8 mb for α_0 and 6.5 ± 2.6 mb for α_1. The experimental results suggest that the reactions proceed mainly by direct-interaction mechanisms. The similarity of the angular distributions of the $Be^9(Li^6,\alpha)B^{11}$ and the $Be^9(He^3,p)B^{11}$ reactions is pointed out.

EXPERIMENTAL INVESTIGATION OF PARITY CONSERVATION IN THE 14.4-kev GAMMA TRANSITION IN Fe^{57}. Lee Grodzins and Frank Genovese, Laboratory for Nuclear Science, Massachusetts Institute of Technology, Cambridge, Massachusetts (Received August 23, 1960).

An experiment using recoilless resonance scattering on the 14.4-kev $M1$ gamma rays of Fe^{57} was performed to set a limit on the degree of parity impurities in the nuclear states involved. The anisotropies of the $\Delta M=\pm1$ gamma-ray transition rates were examined towards and away from the direction of nuclear polarization. The use of recoilless resonance scattering allows the problem to be so overdetermined that instrumental anisotropies could be cancelled by appropriate summing of data. No parity-nonconserving anisotropy was observed. Taking into account the slowness of the $M1$ transition compared to a parity-admixed $E1$ transition of single-particle speed, a factor of 100 in amplitude, the limit of $\mathfrak{F}$, the relative strength of a parity-admixed wave function, in this experiment is $\mathfrak{F}\leq10^{-5}$.

INELASTIC SCATTERING OF N^{14} BY C^{12}. M. L. Halbert and A. Zucker, Oak Ridge National Laboratory, Oak Ridge, Tennessee (Received August 18, 1960).

Inelastic scattering of N^{14} by carbon was studied at 27.3 Mev using two surface-barrier counters to detect both the scattered and the recoil particle in coincidence. The cross section for excitation of C^{12} to the first excited state (4.43 Mev) varies only slightly with angle and averages about 0.5 mb/sr. This is about 15 times greater than the theoretical cross section for Coulomb excitation. The cross sections for

scattering to the second, third, and fourth excited states in N^{14} were found to be only 15 to 25% of that for the 4.43-Mev excitation in C^{12}. Scattering to the first excited state of N^{14} was not observed, which is consistent with conservation of isotopic spin.

PROPERTIES OF FINITE NUCLEI. K. A. Brueckner, University of California, La Jolla, California, A. M. Lockett, Los Alamos Scientific Laboratory, University of California, Los Alamos, New Mexico, and M. Rotenberg, University of Chicago, Chicago, Illinois (Received August 26, 1960).

The properties of O^{16}, Ca^{40}, and Zr^{90} have been determined, using the Brueckner-Gammel-Weitzner theory of finite nuclei. Self-consistent solutions of the Hartree-Fock equations as modified by Brueckner and Goldman have been obtained. The properties computed include binding energy, mean proton and neutron radii, separation energies, spin-orbit splittings, nonlocal and state-dependent single-particle potentials, surface depth of density and potentials, and potential-density relation. The predictions of the theory are in semiquantitative agreement with experiment.

DYNAMICS OF INTERNALLY CONVERTED ELECTRON-POSITRON PAIRS. N. P. Samios, Columbia University, New York, New York, and Brookhaven National Laboratory, Upton, New York (Received August 19, 1960).

The reactions studied were $\pi^- + p \rightarrow n + \pi^0$ ($\pi^0 \rightarrow \gamma + e^+ + e^-$) and $\pi^- + p \rightarrow n + e^+ + e^-$. From a sample of ~15 000 internally converted electron-positron pairs, 7000 were measured, of which 4200 were used in the detailed analysis. The differential distributions in y (the energy partition) and x^2 (the virtual mass of the photon) agree with the theoretical quantum electrodynamic calculations. A measure of the form factor for the $\pi^0 \rightarrow 2\gamma$ reaction gave $\Gamma(x/\mu) = 1 - (0.24 \pm 0.16)x^2/\mu^2$, where μ is the mass of the pion. It was further demonstrated that the number of events necessary to determine the contribution of the longitudinally polarized virtual γ rays in the second reaction is of the order of 50 times that in the present experiment.

DEPOLARIZATION OF NEGATIVE μ MESONS. R. A. Mann* and M. E. Rose, Oak Ridge National Laboratory, Oak Ridge, Tennessee (Received August 22, 1960).

The depolarization of negative μ mesons is discussed in terms of the processes occurring in the formation of μ-mesonic atoms and the subsequent cascade to the ground state. The initial distribution of μ mesons in capturing states of carbon is deduced. The depolarization due to the capture process is derived in a fashion free of essentially all approximations. The only assumption involved is that the scattering cross section is such as to randomize the direction of motion prior to capture and this assumption is shown to be well fulfilled. The effect of radiative transitions in producing depolarization is determined with all possible dipole transitions taken into account. Only nuclei with zero spin are treated in detail. The Auger process is included in a schematic fashion which is sufficient for the purpose in hand. It is shown that both radiative and Auger transitions must be included in the discussion of the depolarization processes in the cascade. The theoretical results are compared with experiment, and from the comparison it is concluded that the observed facts are well accounted for.

*Present address: Department of Physics, University of Alabama, University, Alabama.

SCATTERING OF HIGH-ENERGY ELECTRONS FROM Ca^{40}, V^{51}, Co^{59}, In^{115}, $Sb^{121,123}$, AND Bi^{209}. H. Crannell, R. Helm, H. Kendall, J. Oeser, and M. Yearian,* Department of Physics and High-Energy Physics Laboratory, Stanford University, Stanford, California (Received August 22, 1960).

The absolute elastic electron-scattering cross sections of Ca^{40}, V^{51}, Co^{59}, In^{115}, $Sb^{121,123}$, and Bi^{209} have been measured at a number of angles at a primary electron energy of 183 Mev. The cross sections were obtained by comparison with scattering from the proton. These data have been compared with the previous relative angular distributions measured by Helm, Ravenhall, and Hofstadter. The present data are in closer agreement with the charge distributions found from fitting a Fermi two-parameter model to the older data than with those found from a fit of the Ford and Hill charge distributions.

The absolute cross sections for Bi^{209} show the least agreement: They are 35% larger than the predictions of the Fermi model and about 70% larger than the Ford and Hill model.

*Now at the University of Pennsylvania, Philadelphia, Pennsylvania.

EFFECTS OF THE PION-PION RESONANCE AND THE THREE-PION RESONANCE OR BOUND STATE ON NEUTRAL-PION DECAY. How-sen Wong,* Lawrence Radiation Laboratory, University of California, Berkeley, California (Received July 27, 1960; revised manuscript received September 28, 1960).

We have applied the dispersion method to the problem of neutral-pion decay. It is shown that a pion-pion P-wave resonance can produce a large effect in the decay matrix element. The contribution is related to the semifundamental constant which determines the rate of photoproduction of pions from pions. The contribution of a strong three-pion state is also considered.

*Now at Laboratory of Nuclear Studies, Cornell University, Ithaca, New York.

MASS AND LIFETIME OF UNSTABLE PARTICLES. R. Jacob and R. G. Sachs, University of Wisconsin, Madison, Wisconsin (Received August 19, 1960).

The relationship between the properties of the propagator of an unstable particle and the observation of mass and lifetime is considered. For illustrative purposes a model of a scalar (or pseudoscalar) particle (θ) weakly coupled to two pions is treated. The propagator is shown to have a simple pole on the second (unphysical) Riemann sheet and it is assumed, as suggested by Peierls, that this is generally the case. By analysis of a prototype experiment in terms of wave packets, it is shown that the measured mass and lifetime are determined by the real and imaginary parts of the pole, respectively. Nonexponential terms occur in the lifetime curve, as is well known. These are shown to be related to the uncertainty in the time of the production or detection event under normal circumstances. This conclusion is similar to those of Lévy and of Schwinger, but more closely related to experimental conditions. In particular it is found that the wave packets introduce a "mass filter" in a somewhat different manner from that suggested by Schwinger.

Under special conditions a $t^{-\frac{3}{2}}$ term may occur in the amplitude but would be unimportant in magnitude for, say, the decay of a strange particle. It is noted that such nonexponential decay curves might occur for certain low-energy nuclear processes.

Consideration is also given to the treatment of two degenerate, unstable particles, such as the neutral K mesons. The general method for handling the problem leads, in the weak-coupling limit, to the same result as the Wigner-Weisskopf method.

NOON-MIDNIGHT RED SHIFT. Banesh Hoffmann, Queens College, Flushing, New York (Received June 17, 1960; revised manuscript received September 7, 1960).

A terrestrial atomic clock at noon can be some 10^9 cm nearer the sun than an antipodal clock at midnight. The difference in gravitational potential due to the sun corresponds to a difference of time rates corresponding to a red shift $\Delta\nu/\nu = 8\times10^{-13}$. But this red shift is almost exactly cancelled by a violet shift arising from the relativistic Doppler effect, so that the resultant shift is essentially zero. If the earth shielded or focussed the solar gravitational field, the gravitational contribution to the red shift would be altered and one might expect a resultant shift. But the motional contribution to the shift is also altered and, except for unrealistically large shielding or focussing, the resultant shift would still be zero.

However, all this is true only if the principle of equivalence is valid. The Pound-Rebka experiment confirms its local validity with a 10% accuracy. A 10% discrepancy could imply a noon-midnight red shift $\Delta\nu/\nu = 8\times10^{-14}$ compared with 5×10^{-16} in the Pound-Rebka experiment. Moreover, since the solar gravitational contribution to the value of g is only $5\times10^{-4}g$, the Pound-Rebka experiment is insensitive to solar effects and would not detect possible anomalies arising from shielding or focussing by the earth of the locally almost uniform solar gravitational field which might nevertheless affect the noon-midnight shift. Detection of a significant noon-midnight shift would be a disproof of the general theory of relativity.

SOME SINGULARITIES OF SCATTERING AMPLITUDES ON UNPHYSICAL SHEETS. J. Gunson and J. G. Taylor, Department of Applied Mathematics and Theoretical Physics, University of Cambridge, Cambridge, England (Received August 25, 1960).

An investigation of the consequences on unphysical sheets of a Mandelstam-type representation holding for a two-particle scattering amplitude on the physical sheet is described. The domain of analyticity in the energy and momentum transfer variables is constructed and compared with perturbation theory. A theorem on multiplication of singularities for Legendre polynomial expansions used in our discussion is proved.

DIVERGENCE OF THE GREEN'S FUNCTION SERIES FOR REARRANGEMENT COLLISIONS. Ronald Aaron, Ralph D. Amado, and Benjamin W. Lee, Department of Physics, University of Pennsylvania, Philadelphia, Pennsylvania (Received June 29, 1960; revised manuscript received September 26, 1960).

The convergence of the Born series for rearrangement collisions is investigated in a potential model. For a certain class of potentials it is shown that the iterated series for the full two-particle Green's function, $(\vec{k}_1'\vec{k}_2'|G(E)|\vec{k}_1\vec{k}_2)$, in terms of either the free-particle Green's function, the initial-state Green's function, or the final-state Green's function diverges for some continuous range of the variables $\vec{k}_1$, $\vec{k}_2$, $\vec{k}_1'$, and $\vec{k}_2'$ independent of the energy, E, of the incident particle. It is suggested that the usual Born series, which is an integral over this Green's function series, therefore, also diverges for rearrangement collisions independent of the incident energy.

NONLEPTONIC DECAY MODES OF THE HYPERONS. G. Feldman,* P. T. Matthews, and A. Salam, Imperial College, London, England (Received July 11, 1960).

An attempt is made to correlate the observed asymmetries in hyperon decays and the hyperon decay times using a pole approximation to the decay matrix elements. It is found that a natural correlation is obtained if a near-global relation between pion coupling constants is assumed.

*On leave from The Johns Hopkins University, Baltimore, Maryland.

TOTAL COMPTON CROSS SECTION FOR ARBITRARY SPIN. C. G. Bollini, Department of Mathematics, Imperial College, London, England (Received July 25, 1960).

The magnitude of the total Compton cross section for arbitrary spin is calculated in lowest order by using the absorptive part of the forward scattering amplitude and the unitarity property of the S matrix. To find the general form (for any spin) of the forward amplitude a universal electromagnetic interaction, implying the value 2 for the gyromagnetic ratio, is postulated. The deduced cross section contains as special cases the known cross sections for spinless and Dirac particles. The average of the cross section over all the possible polarization states of the particle is also determined. In the high-energy region the cross section never increases faster than linearly with the energy of the photon. If a development in powers of the photon energy is made, the first and second coefficients are found to be spin independent. The coefficient of the square of the energy is proportional to the square of the modulus of the spin vector.